Overexpression of Mammalian *Nanog* mRNA Hyperdorsalises Zebrafish Embryos

Ying Jiang

Girton College

University of Cambridge

Wellcome Trust Sanger Institute

December 2010

Thesis Presented for the Degree of Master of Philosophy

Table of contents

Abbreviations

PGCs   primordial germ cells

ES cells   embryonic stem cells

LIF   leukemia inhibitory factor

hsnanog   human *NANOG* cDNA

mnanog   mouse *Nanog* cDNA

hsnanog-pCS2+   recombinant construct of human

                                          NANOG cDNA subcloned into pCS2+

mnanog-pCS2+   recombinant construct of mouse

                                          Nanog cDNA subcloned into pCS2+

reverse transcription polymerase chain reaction   RT-PCR

microlitre   μl

nanogram   ng

milligram   mg

Tris-acetate-EDTA Buffer   TAE Buffer

deoxyribonuclease I   DNase I

dithiothreitol   DTT

New England Biolabs   NEB

Abstract

The work presented in this thesis is an investigation of the effects of misexpression of mammalian *NANOG/Nanog* mRNA in zebrafish embryos. I measured whether there was any effect of overexpression of mammalian *NANOG/Nanog* mRNA on the specification of germ line and on dorsal-ventral patterning. I subcloned human *NANOG* and mouse *Nanog* cDNAs into the pCS2+ vector for in vitro transcription, synthesized RNA and injected embryos. I then observed changes in the morphology of zebrafish embryos and counted the number of primordial germ cells. I used quantitative RT-PCR to quantify expression of five genes involved in dorsal-ventral patterning, and used a t-test to determine the significance of gene expression changes. The results show that the overexpression of either human *NANOG* mRNA or mouse *Nanog* mRNA by injection leads to significantly dorsalized changes in the morphology of the zebrafish embryos (25% and 56% of embryos show significant changes in their morphology after injection with 50 pg and 100 pg human *NANOG*; 81% and 82% of embryos show significant changes after injection with 50 pg and 100 pg mouse *Nanog*). I could detect no difference in the number of primordial germ cells between control and *NANOG*-injected embryos. I found, however, that expression of *goosecoid* was significantly upregulated and expression of *wnt8a* was significantly downregulated in *NANOG/Nanog*-injected embryos, which is consistent with the dorsalized phenotypes of *NANOG/Nanog*-injected embryos.

Preface

This thesis is the result of my own work and not the product of any collaboration. Other scientific results are referenced throughout the body of this thesis and in a bibliography. This thesis is not substantially the same as any that I have submitted for a degree or diploma or other qualification at any other University.

Acknowledgements

CHAPTER 1 Introduction

1.1 Transcription factors and Nanog

Transcription factors control the transfer of genetic information from DNA to mRNA and are essential for regulation of gene expression in many important biological processes (Karin, 1990; Latchman, 1997). Genes are upregulated or downregulated by transcription factors through their binding to specific sequences of DNA by different kinds of mechanisms, including inhibiting RNA polymerase from binding to DNA, catalyzing biochemical modifications of histone proteins, and recruiting coactivator or corepressor proteins to the transcription factor complex (Xu et al., 1999; Narlikar et al., 2002).

A homeobox is a DNA sequence first identified in genes regulating anatomical development in *Drosophila* (McGinnis et al., 1984; Scott and Weiner et al., 1984). The homeobox encodes a highly conserved helix-turn-helix protein domain, the homeodomain, which can bind DNA when expressed (Tullius, 1995). Homeobox genes encode transcription factors which switch on expression of downstream genes (Liang and Biggin, 1998). One class of homeobox genes is *Hox* genes, which specify the anterior-posterior axis and segment identity (Wellik, 2009; Alexander et al., 2009; Iimura et al., 2009). *Antennapedia* in *Drosophila* can cause development of legs instead of antennae (Postlethwait and Schneiderman, 1969). Other classes of homeobox genes include *Barx1*, *Msx1* and *Nkx2* (Hill et al., 1989; Kim and Nirenberg, 1989; Tissier-Seta et al., 1995; Harvey, 1996).

The *Nanog* gene was first isolated by Dr. Ian Chambers et al. (2003) and derives its name from the mythological Celtic land of the ever-young Tir nan Og (Chambers et al., 2003;

Mitsui et al., 2003). It encodes a homeodomain-containing transcription factor found in embryonic stem cells, which plays an important role in sustaining pluripotency (Chambers et al., 2003; Mitsui et al., 2003). It enables embryonic stem cells to produce any somatic cell type or primordial germ cells (Chambers et al., 2003; Mitsui et al., 2003; Chambers et al., 2007), and functions with other transcription factors to maintain embryonic stem cell identity (Nichols et al., 1998; Niwa et al., 2000; Avilion et al., 2003; Chambers and Tomlinson, 2009). Mouse Nanog and human NANOG proteins consist of a Serine-rich N-terminal motif, a homeodomain, and a Tryptophan-rich C-terminus (Chambers et al., 2003; Mitsui et al., 2003). The homeodomain region plays an important role in binding DNA sequences (Tullius, 1995). A maximum of 50% amino acid identity is found over the homeodomain of Nanog with Barx1, Msx1 and members of the NK-2 family (Hill et al., 1989; Kim and Nirenberg, 1989; Tissier-Seta et al., 1995; Harvey, 1996; Chambers et al., 2003). The *Nanog* homeobox is closest to that of the *NK-2* gene family (Kim and Nirenberg, 1989; Harvey, 1996; Mitsui et al., 2003). However, mouse Nanog and human NANOG have valine instead of tyrosine in a conserved position in the homeodomain (Harvey, 1996; Mitsui et al., 2003). Mouse Nanog and human NANOG lack the TN and SD domains, which are conserved in members of the NK-2 family (Harvey, 1996; Mitsui et al., 2003). In addition, the Tryptophan-rich domain (WR domain) in mouse Nanog and human NANOG mediates dimerization (Mullin et al., 2008; Wang et al., 2008).

Overexpression of *Nanog* in mouse embryonic stem cells causes them to self renew in the absence of leukemia inhibitory factor (LIF) (Chambers et al., 2003; Mitsui et al., 2003). Aside from ES cells, Nanog is found in mammalian pluripotent cells and developing germ cells (Chambers et al., 2003; Mitsui et al., 2003). The inner cell mass with *Nanog* deleted fails to mature into pluripotent epiblast, suggesting that Nanog is indispensable for constructing the inner cell mass state (Mitsui et al., 2003; Silva et al., 2009). *Nanog* is

7

expressed in mouse germ cells during the period of epigenetic erasure and germ line commitment (Yamaguchi et al., 2005) and is thought to mediate germline development (Chambers et al., 2007). It is essential for PGCs to complete colonizing the genital ridge (Chambers et al., 2007). Embryonic stem cells with *Nanog* disrupted can contribute to the germ line but *Nanog*-deficient primordial germ cells stay in the soma rather than migrating to the genital ridge beyond E11.5 (Chambers et al., 2007). It suggests that Nanog has an essential function in construction of the germ cell state (Chambers et al., 2007).

Among numerous transcription factors, some factors have been of recent interest because of their ability to cause otherwise differentiated cells to become pluripotent (Hanna et al., 2010). These induced pluripotent stem cells (iPS) are derived from somatic cells by introducing a defined set of genes (Hanna et al., 2010). They were first generated by Takahashi and Yamanaka in 2006, who used retroviruses to transfect mouse fibroblasts with a selection of genes considered important for embryonic stem cell maintenance. Transgenic expression of these transcription factors has been used to generate induced pluripotent stem cells from human and mouse somatic cells (Takahashi and Yamanaka, 2006; Takahashi et al., 2007; Yu et al., 2007). Different methods have been used to introduce transcription factors into somatic cells, including retroviral, lentiviral, adenoviral and plasmid transfection (Stadtfeld and Hochedlinger, 2010). These reprogrammed cells are similar to ES cells in their morphology, expressing ES cell marker genes, and forming tumours when injected into mice (Takahashi and Yamanaka, 2006; Takahashi et al., 2007; Yu et al., 2007).

In embryonic stem cells, Nanog, along with Oct3/4 and Sox2, is necessary to promote pluripotency (Nichols et al., 1998; Niwa et al., 2000; Avilion et al., 2003; Chambers et al., 2003；Mitsui et al., 2003). Research by Yu et al. (2007) shows that NANOG is one of the four factors (OCT4, SOX2, NANOG and LIN28) that are sufficient to reprogram human

somatic cells to pluripotent stem cells, which exhibit the essential characteristics of embryonic stem (ES) cells. Aside from the work of Yu et al. in 2007, Takahashi and Yamanaka have tested twenty four factors that maintain pluripotency in embryonic stem cells as initial candidates of key factors inducing pluripotency in somatic cells in 2006. As a result, four factors, Oct3/4, Sox2, Klf4 and c-Myc, were found to be sufficient in reprogramming mouse fibroblasts (Takahashi and Yamanaka, 2006).

It is meaningful to study these important transcription factors including Nanog and induced pluripotent stem cells as they have great potential for biomedical research, disease research and toxicology (Yamanaka, 2009).

Aside from mouse and human, orthologues of *Nanog* have been identified in chick and axolotl (Lavial et al., 2007; Dixon et al., 2010). At the time we started the work, we were not aware of Zgc: 193933 as a potential zebrafish *nanog*, so we decided to work with human *NANOG* and mouse *Nanog* cDNAs. Although recently a *Nanog* homolog has been cloned from medaka and a potential zebrafish *nanog* (Zgc: 193933) has been identified, the similarity is overall very low compared with human *NANOG* and mouse *Nanog* (Chambers et al., 2003 ; Mitsui et al., 2003; Camp et al., 2009). Moreover, the putative Nanog homeodomain protein in medaka has not been found to regulate pluripotency in ES cells as mammalian NANOG/Nanog, chicken Nanog and axolotl Nanog do (Chambers et al., 2003; Mitsui et al., 2003; Lavial et al., 2007; Dixon et al., 2010). Additionally, human *NANOG*, mouse *Nanog* and chicken *Nanog* enable LIF-independent self-renewal when overexpressed in mouse ES cells, which medaka *Nanog* has not been found to be able to (Chambers et al., 2003; Mitsui et al., 2003; Lavial et al., 2007; Dixon et al., 2010). Axolotl *Nanog* overexpression in mouse embryonic stem cells cannot support self-renewal in the absence of LIF, but its homodimer generated with WR domain inserted is able to rescue LIF-

independent self-renewal (Dixon et al., 2010). There are no studies on the activity of the potential zebrafish *nanog* (Zgc: 193933) to justify it as an orthologue of *Nanog*.

1.2 Overexpression of mammalian *NANOG/Nanog* mRNA in zebrafish embryos

During animal development, the germ line serves an important role producing gametes and offspring. Primordial germ cells are stem cells that give rise to the gametes. In many animals, primordial germ cells originate near the gut and migrate to the developing gonads. In the gonads, they undergo mitosis and meiosis as they differentiate into mature gametes. There are different ways of generating the germ line, and one way of germ line formation is by induction (Saffman and Lasko, 1999). In mammals primordial germ cells are induced from epiblast (Ying et al., 2001), and in axolotls they can be specified from primitive ectoderm in response to inducing signals (Sutasurya and Nieuwkoop, 1974; Johnson et al., 2003). It has been proposed recently that ground state pluripotency giving rise to any somatic cell type or primordial germ cells is conserved from urodele amphibians to mammals (Dixon et al., 2010). In zebrafish and frogs, however, primordial germ cells are specified by genetic determinants inherited from maternal stores (Ikenishi et al., 1974; Zust and Dixon, 1975; Houston and King, 2000; Raz, 2002; Raz, 2003).

1.2.1 Germ line development in mammals

In mammals primordial germ cells are induced from pluripotent epiblast cells by signals controlled by zygotic genes of neighbouring cells (Ying et al., 2001; Ying et al., 2002; Saga, 2008).

Early specification of mouse primordial germ cells is completed by induction of regulators including Blimp1 and Bmps such as Bmp2, Bmp4 and Bmp8b (Lawson et al., 1999; Ying et al., 2001; Ying and Zhao, 2001; Saga, 2008). Migration of mouse primordial germ cells relies on receptor-ligand interactions, for example the *C-kit* receptor expressed in the PGCs and its ligand *Steel* expressed by somatic cells along the migratory route (Matsui et al., 1990; Bernex et al., 1996). They are also guided towards the genital ridge by long-distance signalling (Godin et al., 1990). In addition, PGC migration is guided by the interaction between PGCs and extracellular matrix molecules such as Beta1 integrins (Anderson et al., 1999). In mouse, primordial germ cells lacking *Nanog* cannot mature on reaching the genital ridge (Chambers et al., 2007).

1.2.2 Germ line development in zebrafish

In zebrafish, germ line specification occurs in cells that inherit germ plasm from maternal stores (Raz, 2002; Raz, 2003). During the zygote period, maternal germline determinants are located in a special type of cytoplasm, the germ plasm. During early cleavage stages, zebrafish germ plasm is first divided into four blastomeres. The germ plasm in each blastomere is then asymmetrically distributed into only one daughter cell during cell divisions. The cytoplasmic determinants specify primordial germ cells at the late blastula stage.   In subsequent divisions of primordial germ cells, germ plasm is symmetrically distributed into

both daughter cells (Yoon et al, 1997; Braat et al., 1999; Knaut et al., 2000; Raz, 2002; Raz, 2003). Primordial germ cells go through six steps of migration in the first 24 hours post fertilization (Weidinger et al., 1999). They are first attracted towards an intermediate target and then migrate to the final target, the gonads (Weidinger et al., 2002).

Zebrafish *vasa* is a germ cell-specific gene and its transcript is a marker for zebrafish germ line. Zebrafish *vasa* RNA is a component of germ plasm and segregates asymmetrically during early cleavage stages. Zygotic *vasa* transcription starts after germ plasm segregation pattern changes (Yoon et al., 1997; Braat et al., 1999; Knaut et al., 2000).

Another important component of zebrafish germ plasm is *nanos* RNA. Similar to *vasa* RNA, maternal *nanos* RNA degrades in somatic cells but specifically stabilizes in PGCs, enabling specific expression of *nanos* in PGCs. Moreover, zygotic Nanos protein is essential for migration and survival of PGCs in zebrafish (Köprunner et al., 2001).

1.2.3 Zebrafish Development

Zebrafish, *Danio rerio*, is an important model organism in developmental studies. The embryo of the zebrafish goes through several periods including zygote, cleavage, blastula, gastrula, segmentation, pharyngula, hatching and early larva in the first three days after fertilization. Cytoplasm streams toward the animal pole and forms blastodisc which is incompletely cleaved into interconnected blastomeres. As the number of blastomeres increases, cell cycles lengthen asynchronously when the embryo enters midblastula transition, and the blastodisc spreads over the yolk, which is completely engulfed at the end of gastrula period. The somites develop during segmentation period. The embryo completes most processes of morphogenesis, cell growth and cell differentiation at the end of hatching period.

The early larva continues to grow rapidly, go through changes such as inflation of the swim bladder and begins to swim about actively (Kimmel et al., 1995).

1.2.4 Dorsal-Ventral Patterning

Dorsal-ventral patterning is an important stage of early zebrafish development. Dorsal-ventral pattern formation is regulated by the opposing effect of ventralizing genes such as the *bmp* gene family (Nikaido et al., 1997) and the *wnt* gene family (Kelly et al., 1995; Lekven et al., 2001; Ramel and Lekven, 2004), and dorsal-specific genes such as *chordin* (Schulte-Merker et al., 1997). Bone morphogenetic proteins (BMPs) are key mediators of dorsal-ventral patterning and are required for the induction of ventral fates in fish and frogs (Nikaido et al., 1997; Schmid et al., 2000). Ventral genes such as *gata1* and the *bmp* genes themselves are activated by BMP signalling (Kishimoto et al., 1997; Schmid et al., 2000; Stickney et al, 2007). A BMP activity gradient, which forms by the interaction between BMPs and BMP antagonists, patterns cell fates along the dorsal-ventral axis (Schier and Talbot, 2005). In this thesis, we use the following five factors which function in dorsal-ventral patterning (Figure 1).

Ventralizing factors   Dorsalizing factors

Bmp2b   Chordin

Wnt8a   Goosecoid
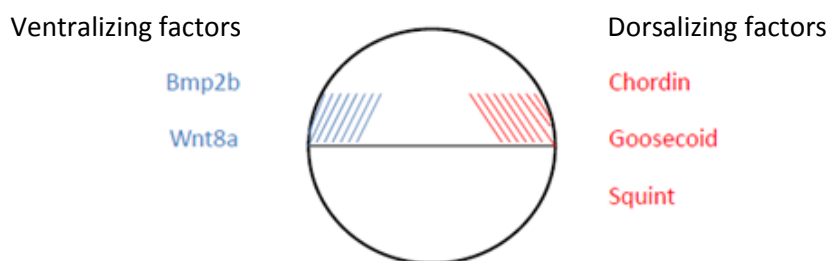
                                         Squint

Figure 1. Some zebrafish dorsoventral patterning factors

An important member of the *bmp* gene family is **bmp2b** (Martínez-Barberá et al., 1997; Nikaido et al., 1997). It functions as an essential gene during early dorsal-ventral patterning in zebrafish, being required for ventral specification (Kishimoto et al., 1997; Nguyen et al., 1998). Overexpression of *bmp2b* causes expansion of ventral gene expression and reduces dorsal structures such as notochord (Nikaido et al., 1997). Previous studies have shown that mutations in the zebrafish *bmp2b* gene cause a dorsalized phenotype (Kishimoto et al., 1997; Nguyen et al., 1998). In the *swirl* mutant, several processes for primordial germ cell migration are affected, leading to a defect in movement of PGCs toward the dorsal side of the embryo (Weidinger et al., 1999).

Aside from *bmp2b*, *bmp4* and *bmp7* are both important members of the *bmp* family (Martínez-Barberá et al., 1997; Nikaido et al., 1997; Dick et al., 2000; Schmid et al., 2000). Zebrafish *bmp7* is essential for ventral cell specification (Dick et al., 2000; Schmid et al., 2000). A strongly dorsalized phenotype, *snailhouse*, was caused by mutations in *bmp7* (Dick et al., 2000; Schmid et al., 2000). Zebrafish *bmp4* is expressed in ventral cells during late blastula and gastrula stages and specifies ventroposterior cell fates (Nikaido et al., 1997; Stickney et al., 2007). Disrupted development of ventral tissues such as ventral tail fin is found in *bmp4^{st72}* mutant embryos (Nikaido et al., 1997; Stickney et al., 2007). The dorsalized phenotypes of *swirl* and *snailhouse* mutant embryos can be rescued by *bmp4* (Nguyen et al., 1998). In addition, the role of BMP signalling in dorsoventral patterning changes as zebrafish development proceeds over different stages (Pyati et al., 2005). It is suggested that in zebrafish *bmp2b* and *bmp7* function in early stages of dorsoventral patterning, while *bmp4* together with *bmp2b* regulates late patterning (Stickney et al., 2007).

Homeobox genes *vox* and *vent* encode ventralizing transcriptional factors in early stages of zebrafish dorsoventral patterning (Kawahara et al., 2000a; Kawahara et al., 2000b; Melby

et al., 2000). Expression of *vox* is detected in all blastomeres at the midblastula transition but is downregulated by the late blastula stage (Kawahara et al., 2000a; Melby et al., 2000). Expression of *vent* is detected ventrally at the late blastula stage (Kawahara et al., 2000b; Melby et al., 2000). The asymmetric distribution of Vox and Vent is established by the interaction with their antagonist Bozozok (Kawahara et al., 2000a; Melby et al., 2000). Overexpression of *vox* or *vent* can ventralize zebrafish embryos probably by repressing dorsal genes such as *squint*, *chordin* and *goosecoid* (Kawahara et al., 2000a; Kawahara et al., 2000b; Imai et al., 2001). In zebrafish, *vox* and *vent* repress dorsal fates of zebrafish redundantly (Imai et al., 2001). Either *vox* or *vent* expression disrupted by antisense morpholinos doesn't lead to any dorsoventral patterning defect, while embryos lacking both *vox* and *vent* display a dorsalized phenotype and an expansion of organizer gene expression (Imai et al., 2001).

Dorsal-specific genes ***chordin*** and ***goosecoid*** are important in dorsoventral patterning, and their expression is dorsally restricted (Stachel et al., 1993; Schulte-Merker et al., 1994; Schulte-Merker et al., 1997). Chordin is a BMP antagonist (Schulte-Merker et al., 1997) and mutations in *chordin* result in a ventralized phenotype (Hammerschmidt et al., 1996). In *chordino* mutant embryos, some PGCs are found in positions posterior to the correct ones, indicating a defect in migration of PGCs (Weidinger et al., 1999). The homeobox gene *goosecoid* was first found in a screen for homeobox genes in a dorsal lip cDNA library of *Xenopus* (Blumberg et al., 1991). It was named *goosecoid* for its similarity with *Drosophila* genes *gooseberry* (Nüsslein-Volhard and Wieschaus, 1980; Nüsslein-Volhard et al., 1984) and *bicoid* (Frohnhöfer and Nüsslein-Volhard, 1986). *Xenopus goosecoid* is important for Spemann's organizer function and microinjection of *goosecoid* mRNA into the ventral side of *Xenopus* embryos induces secondary body axes (Cho et al., 1991). Zebrafish *goosecoid* is expressed on the dorsal side of the embryo and its expression domain defines the prospective shield (Stachel et al., 1993; Schulte-Merker et al., 1994). Lithium treatment causes a

dorsalized phenotype of zebrafish embryos and upregulates *goosecoid* expression (Stachel et al., 1993).

Nodal signals are important factors which induce mesoderm formation and dorsoventral patterning in vertebrate embryos (Zhou et al., 1993; Conlon et al., 1994; Jones et al., 1995; Joseph and Melton, 1997). In zebrafish, a *nodal*-related gene **squint** functions in patterning of mesendoderm (Heisenberg and Nüsslein-Volhard, 1997; Erter et al., 1998; Feldman et al., 2000; Dougan et al., 2003). Dorsal mesoderm structures are reduced in *squint^{cz35}* mutant embryos (Feldman et al., 2000; Dougan et al., 2003). Overexpression of *squint* induces dorsal mesoderm structure such as notochord and somites (Erter et al., 1998). It has been shown that Squint specifies the fate of cells directly at a distance as a morphogen does (Chen and Schier, 2001).

Wnt signalling pathway also plays an important role in dorsal-ventral patterning during early development (Christian et al., 1991; Christian and Moon, 1993; Hoppler et al., 1996; Lekven et al., 2001; Ramel and Lekven, 2004). Expression of *Xenopus wnt*8 is ventrally restricted (Christian et al., 1991; Smith and Harland, 1991; Christian and Moon, 1993). Overexpression of *Xenopus wnt8* in organizer cells after the midblastula stage is found to ventralize these cells and overexpression of a dominant negative form of *Xenopus* wnt8 reduces ventral mesodermal tissues, suggesting that *wnt8* specifies ventral fates (Christian et al., 1991; Smith and Harland, 1991; Christian and Moon, 1993; Hoppler et al., 1996).

Aside from dorsoventral patterning, Wnts function in anterior-posterior patterning of the neurectoderm (McGrew et al., 1995; McGrew et al., 1997; Bang et al., 1999). Overexpression of Wnts can posteriorize neural tissue (McGrew et al., 1995; McGrew et al., 1997; Bang et al., 1999), while interfering Wnt signalling increases the expression of anterior

neural genes and reduces the expression of posterior neural genes (McGrew et al., 1997; Hsieh et al., 1999).

Zebrafish **wnt8a** is a homologue of *Xenopus wnt8* (Kelly et al., 1995). It is required for ventral specification of mesoderm and also anterior-posterior patterning of the neurectoderm (Lekven et al., 2001; Ramel and Lekven, 2004). Embryos homozygous for *Df(LG14)wnt8^{w8}* with the *wnt8* locus removed exhibit defects in dorsal-ventral mesoderm patterning including an expansion of the shield and defects in anterior-posterior neural patterning (Lekven et al., 2001). Zebrafish Wnt8a is thought to antagonize dorsal organizer (Lekven et al., 2001). It has been suggested that Wnt8a repress the dorsal organizer by regulating early expression of the transcriptional repressors Vent and Vox (Ramel and Lekven, 2004).

1.2.5 Project Aims

Zebrafish, *Danio rerio*, is used as an important model organism for many functional studies, especially for the study of early vertebrate development. With previous studies on Nanog's effect on mouse germ line development (Chambers et al., 2007), we hypothesize that Nanog has an equivalent function in promoting zebrafish germ line development. Although a zebrafish *nanog* sequence has been suggested, there are no studies on the activity of this gene (Zgc:193933) (Camp et al., 2009). At the time we began this work we were not aware of Zgc:193933 as a potential *Nanog* orthologue so we decided to work with human *NANOG* amd mouse *Nanog* cDNAs (Chambers et al., 2003; Mitsui et al., 2003; Camp et al., 2009). We therefore introduce mammalian *NANOG*/*Nanog* into zebrafish embryos. With the study of the changes in germline development and in dorsal-ventral patterning after injecting

NANOG/Nanog mRNA into zebrafish embryos, the effects of overexpression of mammalian *NANOG/Nanog* mRNA on zebrafish embryonic development can be studied. Nevertheless, further studies such as gain-of-function experiments in this thesis with the putative zebrafish *nanog* are warranted to take the study of the effects of *Nanog* on specification of germ line and on dorsal-ventral patterning a step further. Loss-of-function studies such as disrupting endogenous expression of the putative zebrafish *nanog* with morpholinos are worthwhile to supplement studying the function of *nanog* in zebrafish germ line specification and dorsoventral patterning.

The study described in this thesis is to introduce humang *NANOG* and mouse *Nanog* mRNA into zebrafish embryos to study the effects of overexpression of mammalian *NANOG*/*Nanog* mRNA on zebrafish germline development and dorsal-ventral patterning. Figure 2 shows the flowchart of the experiment.

Human *NANOG* and mouse *Nanog* mRNA were injected into zebrafish embryos, and were found to cause changes in morphology. However, microinjection of human *NANOG* into zebrafish embryos doesn't lead to significant changes in the number of primordial germ cells. Moreover, it is found that overexpression of human *NANOG* or mouse *Nanog* mRNA hyperdorsalises zebrafish embryos.
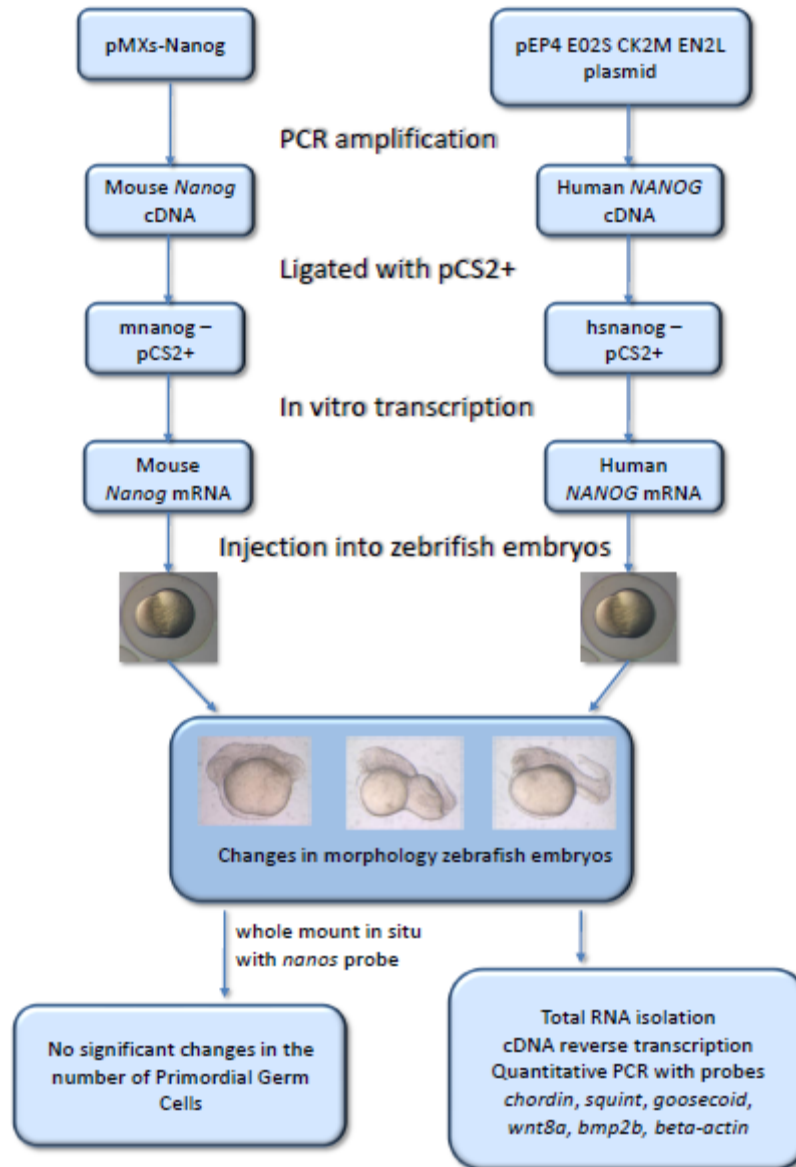
Figure 2. Experimental flowchart

1.3 Chapter Overview

The second chapter discusses PCR amplification of human *NANOG* and mouse *Nanog*, construction of hsnanog-pCS2+ and mnanog-pCS2+ and in vitro transcription of human *NANOG* and mouse *Nanog* mRNA.

The third chapter discusses that injection of human *NANOG* mRNA or mouse *Nanog* mRNA leads to changes in the phenotype of zebrafish embryos but there is no significant change in the number of primordial germ cells.

The fourth chapter discusses total RNA isolation from zebrafish embryos injected with mouse *Nanog* and embryos injected with human *NANOG*, reverse transcription and quantitative RT-PCR assay of expression of five genes involved in dorsal-ventral patterning. It is found that injection of mouse *Nanog* or human *NANOG* mRNA into zebrafish embryos hyperdorsalises zebrafish embryos.

Finally the fifth chapter concludes the work completed in this thesis and discusses what can be done in the future.

CHAPTER 2 Construction of hsnanog-pCS2+ and mnanog-pCS2+ and in vitro transcription of human *NANOG* and mouse *Nanog* mRNA

2.1 Introduction

Among various approaches that can be used to introduce mammalian *NANOG*/*Nanog* into zebrafish embryos, microinjecting *NANOG*/*Nanog* mRNA into the one-cell stage embryo is an efficient and convenient method to study the effects of exogenous *NANOG*/*Nanog* during the developmental time course and is therefore used in this thesis. In order to generate human *NANOG* and mouse *Nanog* mRNA by in vitro transcription, we subcloned human *NANOG* and mouse *Nanog* cDNA into the pCS2+ vector. Vectors pCS2 and pSP64T are generally used for in vitro transcription to generate stably functional mRNAs with 5'- termini GpppG cap and 3'-termini poly-A signal (Krieg and Melton, 1984; Melton et al., 1984). The pCS2+ vector contains a SP6 promoter, multiple cloning sites, and a poly-A signal, allowing RNA polymerase to synthesize messenger RNA of specific DNA template (Krieg and Melton, 1984; Melton et al., 1984; Wu and Alwine, 2004). In this chapter, human *NANOG* cDNA was amplified from the pEP4 E02S CK2M EN2L plasmid (Yu et al., 2009) and mouse *Nanog* cDNA was amplified from the pMXs-Nanog plasmid (Takahashi and Yamanaka, 2006). They were subcloned into the pCS2+ vector to produce constructs of hsnanog-pCS2+ and mnanog-pCS2+, which were subsequently transcribed *in vitro* to synthesize human *NANOG* and mouse *Nanog* mRNA.

2.2 Materials

Special Equipment

NanoDrop	ND-1000 Spectrophotomer
Electrocoating bath	Apollo Instrumentation
Peltier Thermal Cycler	MJ Research
Incubator	
Heat block	

Plasmids

Plasmids carrying human *NANOG* and mouse *Nanog* cDNA

Addgene plasmid 20924: pEP4 E02S CK2M EN2L (Yu et al., 2009)

Addgene plasmid 13354: pMXs-Nanog (Takahashi and Yamanaka, 2006)

The pEP4 E02S CK2M EN2L plasmid and a pMXs-Nanog colony plate were obtained from Wei Wang (Team 18, Wellcome Trust Sanger Institute).

pCS2+
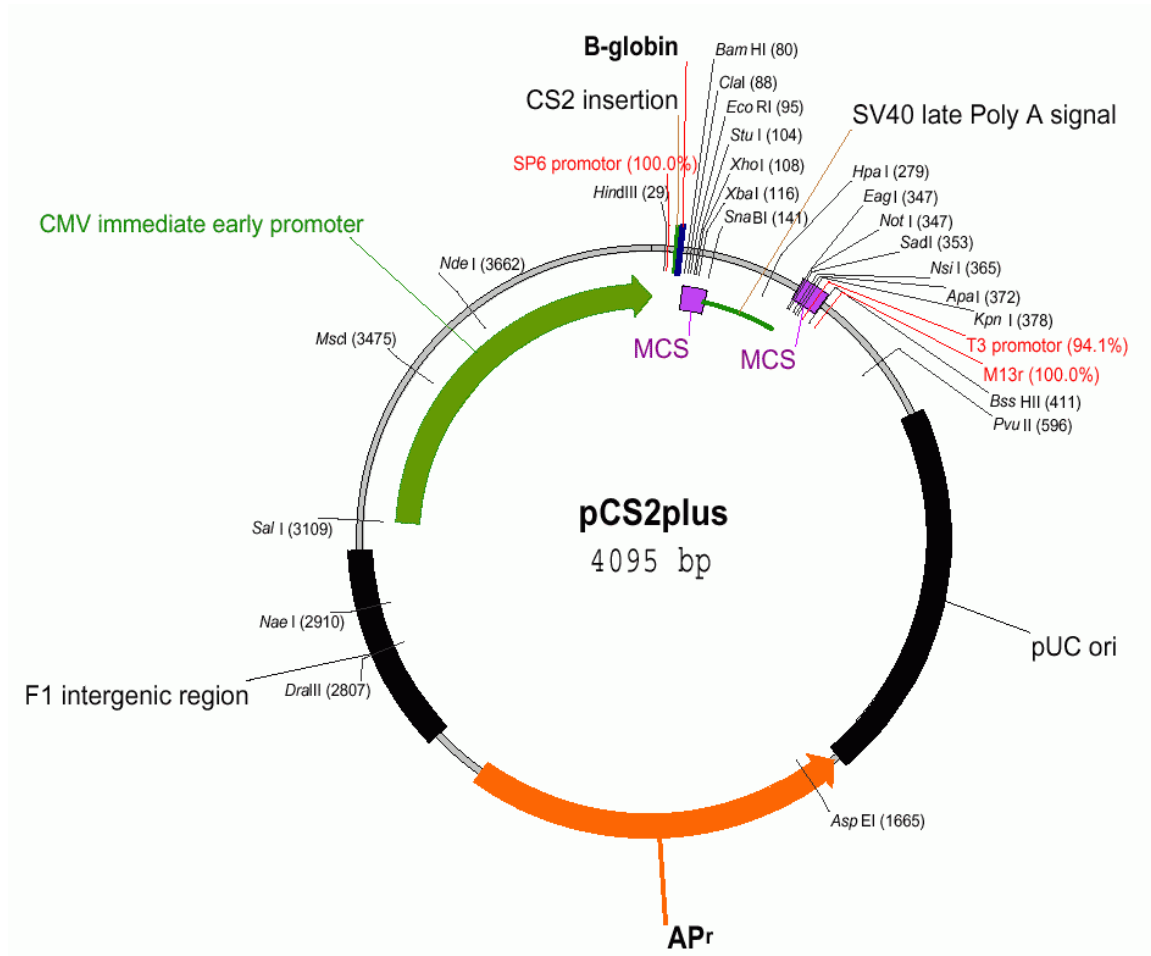
Figure 3. The pCS2+ Vector (www.imagenes-bio.de/info/vectors/pCS2plus.gif)

Recombinant Constructs

hsnanog-pCS2+

Figure 4. Recombinant construct hsnanog-pCS2+.   Between restriction sites of Xho I and Xba I is the human *NANOG* cDNA insert, which is about 900 bp.   Double Digestion of hsnanog-pCS2+ with Xho I and Nco I (New England Biolabs) generates three fragments, which are of approximately170 bp, 690 bp and 4,200 bp.
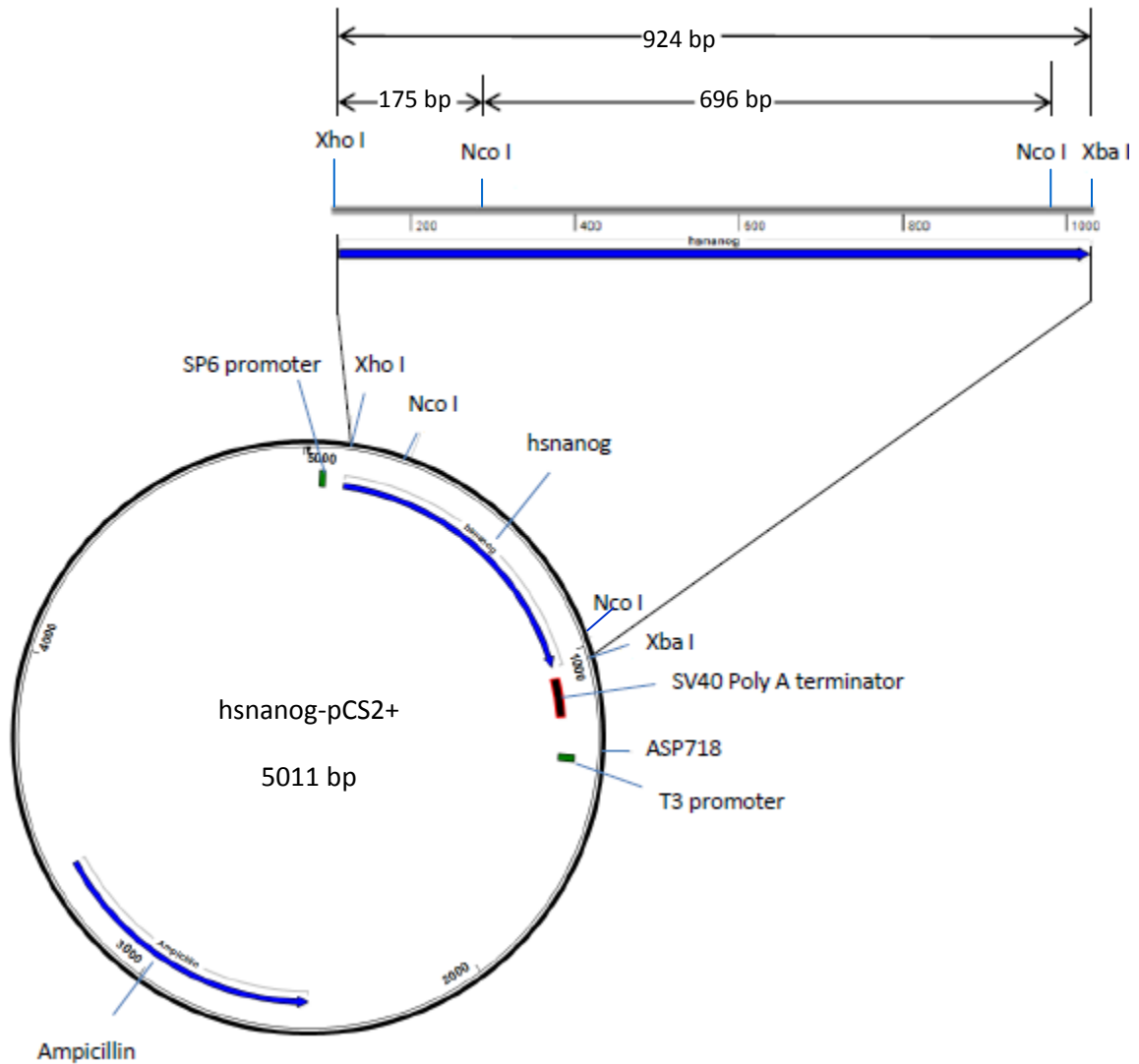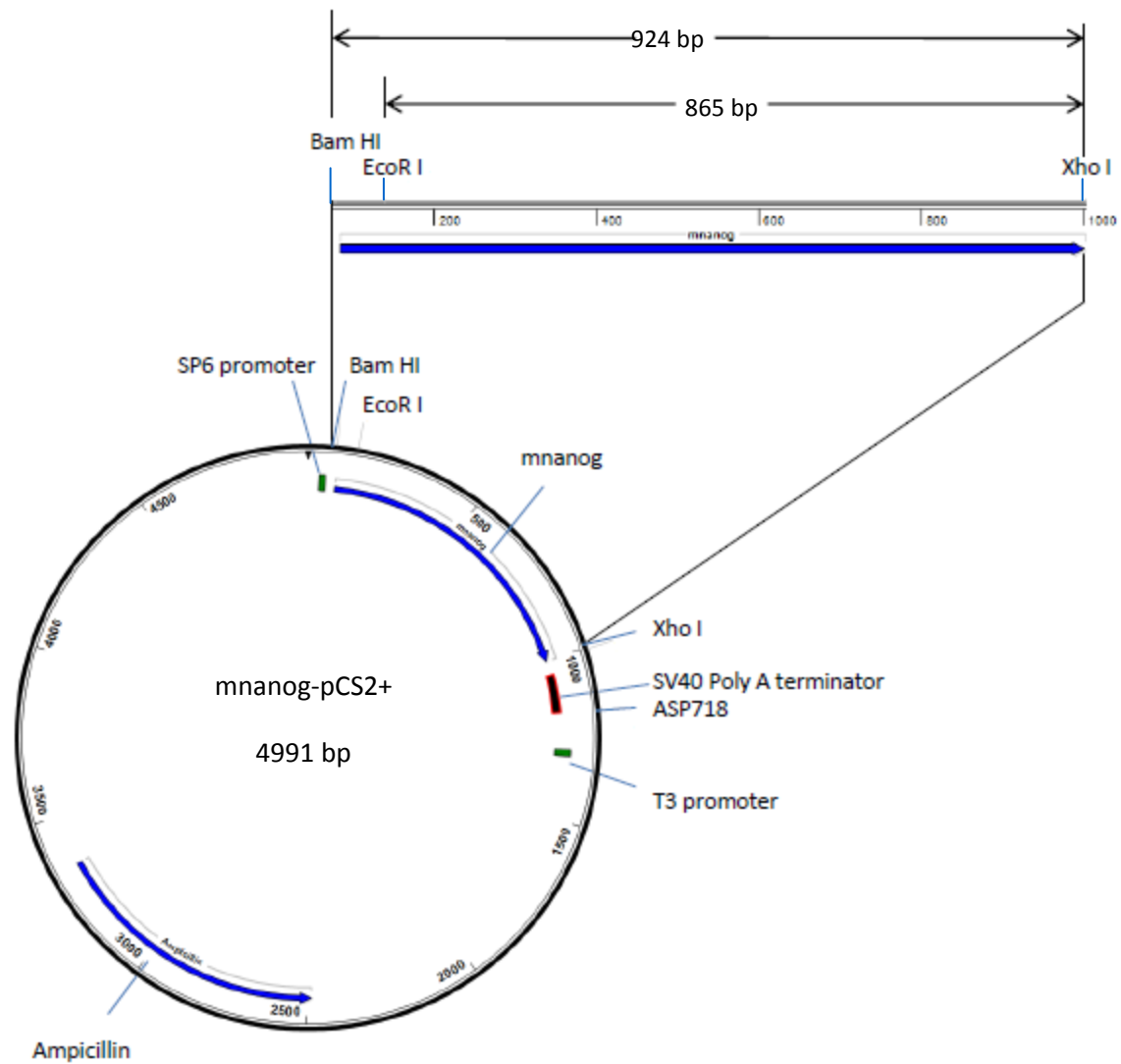
mnanog-pCS2+

Figure 5. Recombinant construct mnanog-pCS2+.   Between restriction sites of Bam HI and Xho I is the mouse *Nanog* cDNA insert, which is about 900 bp.   Double Digestion of mnanog-pCS2+ with EcoR I and Xho I (New England Biolabs) generates two fragment, one of about 860 bp and the other of 4,100 bp.

Primers

Cloning Primers

Human *NANOG* forward primer   5' GTCTCGAGATGAGTGTGGATCCAGCTTGTCC 3'

Human *NANOG* reverse primer   5' CATCTAGATCACACGTCTTCAGGTTGCATG 3'

Mouse *Nanog* forward primer   5' ATGGATCCATGAGTGTGGGTCTTCCTGGTCC 3'

Mouse *Nanog* reverse primer   5'CACTCGAGTCATATTTCACCTGGTGGAGTC 3'

Sequencing Primers

Sequencing Primers of hsnanog-pCS2+

Forward primer   Sp6 promoter 5' ATTTAGGTGACACTAT 3'

Reverse primer   T3 promoter 5' GGGAAATCACTCCCAATTAAC 3'

Sequencing Primers of mnanog-pCS2+

Forward primers   Sp6 promoter 5' ATTTAGGTGACACTAT 3'

                5' GCTGACAAGGGCCCTGAGGAG 3'

                5' ACGGCCAGCCTTGGAATGCTG 3'

Reverse primers   T3 promoter 5' GGGAAATCACTCCCAATTAAC 3'

                5'CATTCCAAGGCTGGCCGTTCC 3'

Kits, enzymes and chemicals

KOD Hot Start PCR Kit	Novagen
QIAquick PCR Purification Kit	Qiagen
QIAquick Gel Extraction Kit	Qiagen
QIAprep Miniprep Kit	Qiagen
Restriction enzymes BstX I, Xho I, Xba I, Nco I, Bam HI, and EcoR I	NEB
Restriction enzyme ASP718	Roche
Quick T4 DNA Ligase	NEB
T4 DNA Ligase	NEB
SP6 RNAPolymerase	NEB
DNase I (RNase-free)	Roche
NEBuffer 3, NEBuffer 4 andNEB EcoR I Buffer	NEB
2X Quick Ligase Buffer	NEB
10X Ligase Buffer	NEB
SURE/Cut Buffer for Restriction Enzyme ASP718	Roche
10X NEB RNA Pol reaction Buffer	NEB
100X BSA	NEB
RNase Inhibitor	NEB
DTT	Promega

rATP, rCTP, rUTP, rGTP and Cap analogue   Promega

Ultra Pure^{TM} Agarose   Invitrogen

DNA marker HyperLadder I and HyperLadder IV   Bioline

Ethidium bromide   10 mg/ml   Sigma

Ampicillin

LB

TAE

Other materials include

CHROMA SPIN^{TM} Columns   Clontech

One Shot TOP 10 Chemically Competent *E.coli*   Invitrogen

Amp Agar Plate

Software

Lasergene (version 8, DNAStar)

2.3 Methods

Construction of hsnanog-pCS2+

Primers were designed to amplify human *NANOG* cDNA from pEP4 E02S CK2M EN2L (Yu et al., 2009) (Materials and Methods Appendix). The PCR product was purified following the QIAquick PCR Purification protocol. Human *NANOG* and pCS2+ were double digested with both Xho I and Xba I, and ligated, generating hsnanog-pCS2+ (Materials and Methods Appendix). Ligation product was used to transform chemically competent *E.coli* following a standard protocol of chemical transformation (One Shot TOP10 Chemically Competent *E.coli* guideline). Six hsnanog-pCS2+ colonies were picked and plasmids were extracted following a standard minipreparation protocol (QIAprep Miniprep Handbook). Diagnostic digest with Xho I and Nco I as well as sequencing were performed to confirm whether the recombinant constructs were correct.

In vitro transcription of human *NANOG* mRNA

Construct hsnanog-pCS2+ was linearized by ASP718 (Materials and Methods Appendix). Human *NANOG* mRNA was generated following a standard protocol of in vitro transcription (Materials and Methods Appendix).

Construction of mnanog-pCS2+

Plasmid pMXS-Nanog was extracted following a standard protocol of minipreparation (QIAprep Miniprep Handbook). Digestion with BstXI was performed to test whether the plasmid pMXS-Nanog was correct (Materials and Methods Appendix). PCR reaction was designed to amplify the mouse *Nanog* cDNA fragment from pMXS-Nanog (Takahashi and Yamanaka, 2006). Mouse *Nanog* and pCS2+ were double digested with both Bam HI and Xho I, ligated and mnanog-pCS2+ were generated (Materials and Methods Appendix). Ligation product was used to transform chemically competent *E.coli* following a standard protocol of chemical transformation (One Shot TOP10 Chemically Competent *E.coli* guideline). Ten mnanog-pCS2+ colonies were picked and plasmids were extracted following a standard protocol of minipreparation (QIAprep Miniprep Handbook). Diagnostic digest with EcoR I and Xho I as well as sequencing were performed to confirm whether the recombinant constructs were correct.

In vitro transcription of mouse *Nanog* mRNA

Construct mnanog-pCS2+ was linearized by ASP718. Mouse *Nanog* mRNA was generated following a standard protocol of in vitro transcription (Materials and Methods Appendix).

2.4 Results

Construction of hsnanog-pCS2+ and in vitro transcription of human *NANOG* mRNA

Correct hsnanog-pCS2+ constructs were made and human *NANOG* mRNA of good quality was generated. Figure 6 illustrates the human *NANOG* cDNA fragment of expected size, which is about 0.9 kb, amplified from pEP4 E02S CK2M EN2L (Yu et al., 2009). Human *NANOG* and pCS2+ were double digested with Xho I and Xba I (Figure 7). Concentration of double digestion products of human *NANOG* and pCS2+ were quantified to be 125.03 ng/µl and 14.19 ng/µl. Therefore the ratio of their volume in the ligation reaction system was decided to be 1: 6.5 (Materials and Methods Appendix). Six colonies were picked from the plate spread with transformed competent *E.coli*. Gel electrophoresis result shows that the six hsnanog-pCS2+ constructs are of good quality (Results Appendix, Figure S1). Double digestion results with Xho I and Nco I show that there are three bands of expected size, about 0.2 kb, 0.7 kb and 4.1 kb, suggesting that all the six hsnanog-pCS2+ clones have human *NANOG* cDNA within them (Figure 8). Sequencing results show that five of them are correct but the other one contain a mutation. Clone 3 was used to generate human *NANOG* mRNA in this chapter. Figure 9 illustrates complete linearization reaction and figure 10 shows RNA of good quality, with two bands of about 600 bp and 900 bp, which represent distribution of RNA conformations.

Figure 6. Gel electrophoresis of human *NANOG*

1, Human *NANOG* cDNA. M, Marker Hyperladder IV. In lane 1 is the human *NANOG* band of expected size, about 900 bp.
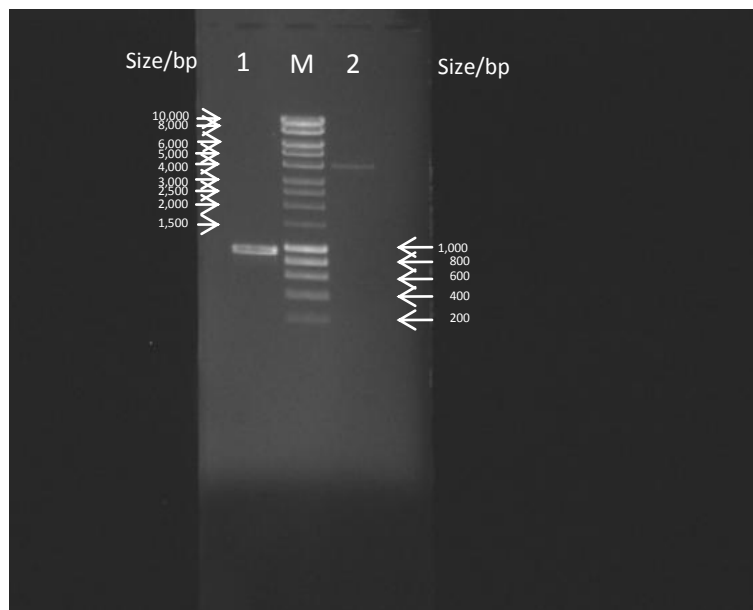
Figure 7. Human *NANOG* and pCS2+ double digested with Xho I and Xba I

1, Human *NANOG* double digested with Xho I and Xba I.

2, pCS2+ double digested with Xho I and Xba I.   M, Marker Hyperladder I.

In lane 1 is the band of human *NANOG* double digested with Xho I and Xba I. Band size is about 900 bp. In lane 2 is the band of pCS2+ double digested with Xho I and Xba I. Band size is about 4,000 bp which is expected for linearized pCS2+.
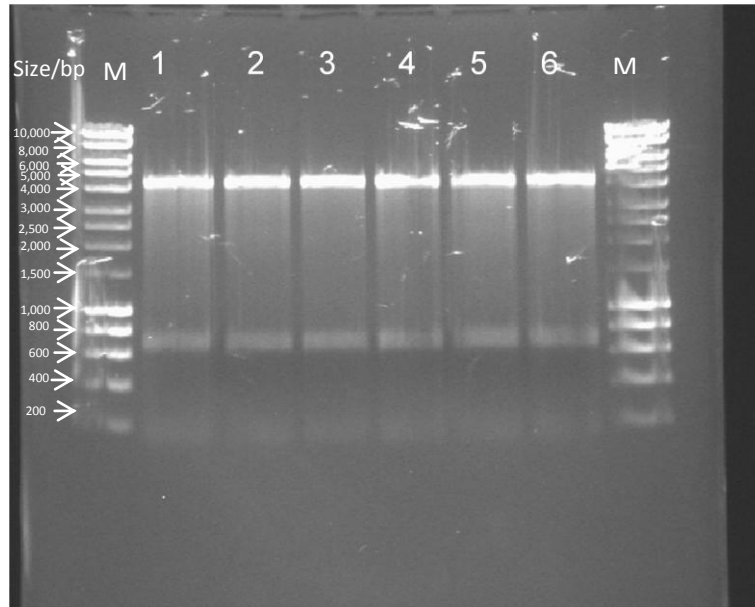
Figure 8. hsnanog-pCS2+ double digested with Xho I and Nco I

1-6, Double digestion of hsnanog-pCS2+ 1-6 with Xho I and Nco I. M, Marker Hyperladder I. There are three bands in each lane. The size of the three bands is about, 0.2 kb, 0.7 kb and 4 kb respectively, which is expected for double digestion of hsnanog-pCS2+ constructs (Figure 5) with Xho I and Nco I, and confirms that all these recombinant constructs contain human *NANOG* inserts.
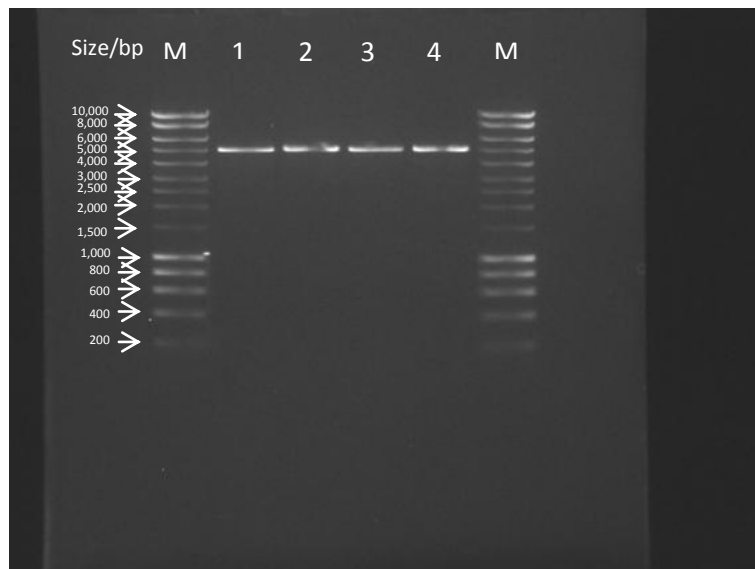
Figure 9. Linearization of hsnanog-pCS2+

1-4, hsnanog-pCS2+ construct 3 linearized by ASP718. M, Marker Hyperladder I. The size of linearised hsnanog-pCS2+ is about 5 kb. The clear single band indicates complete linearization.

Figure 10. Human *NANOG* mRNA

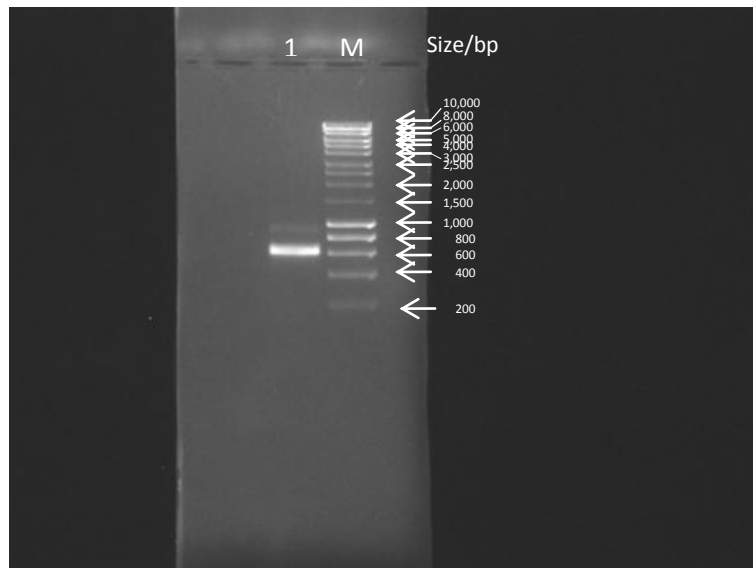1, Human *NANOG* mRNA. M, Marker Hyperladder I. In lane 1 there are two bands. The size of the brighter one is about 600 bp. The size of the other one, which is faint, is about 900 bp.

Construction of mnanog-pCS2+ **and in vitro transcription of mouse** *Nanog* **mRNA**

Correct mnanog-pCS2+ constructs were made and mouse *Nanog* mRNA of good quality was generated. Mouse *Nanog* cDNA of expected size, which is about 900 bp, amplified from pMXs-Nanog (Takahashi and Yamanaka, 2006) is illustrated in figure 11. Figure 12 shows that double digest reaction works well, with one band of about 900 bp for the double digested mouse *Nanog*, and a band of about 4,000 bp as well as a smear of approximately 200 bp for digested pCS2+. The concentration of double digestion products of mouse *Nanog* and pCS2+ were quantified to be 21.69 ng/µl and 12.20 ng/µl. Therefore the ratio of their volume in ligation reaction system was decided to be 1: 1 (Materials and Methods Appendix). Ten colonies were picked from the plate spread with *E.coli* bacteria transformed with ligation product. Gel electrophoresis result shows that these ten mnanog-pCS2+ constructs are of good quality (Results Appendix, Figure S2 and Figure S3). EcoR I and Xho I double digestion result shows that all of them are correct ones because they are cut into two bands, of about 850 bp and 4,000 bp and sequencing results also confirm that clones 1,2,4,6-9 have correct target sequences (Figure 13, Figure 14). Figure 15 and figure 16 show that mnanog-pCS2+ is linearized and mouse *Nanog* mRNA of good quality is generated, with two bands of about 800 bp and 1,000 bp.
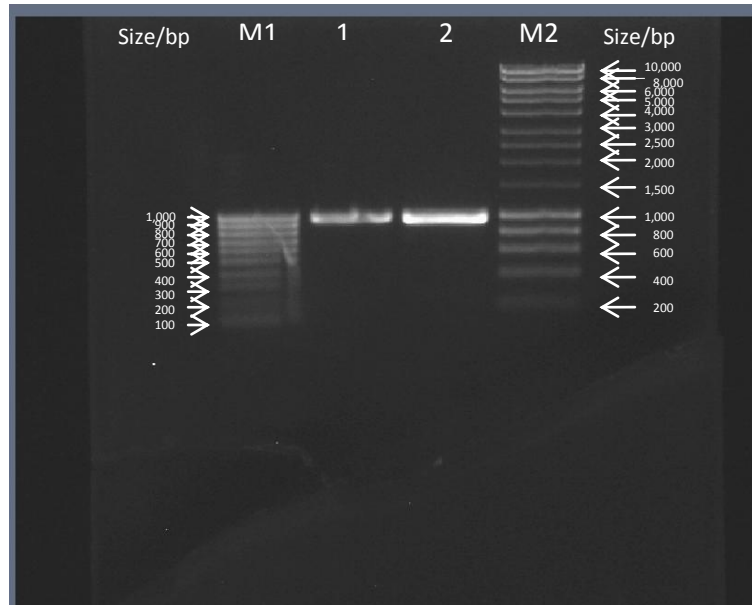
Figure 11. Gel electrophoresis of mouse *Nanog*

M1, Marker Hyperladder IV. M2, Marker Hyperladder I. 1-2, Mouse *Nanog*. In lane 1 and lane 2 is the mouse *Nanog* band of about 900 bp. In lane M1 is marker hyperladder IV. In lane M2 is marker hyperladder I.
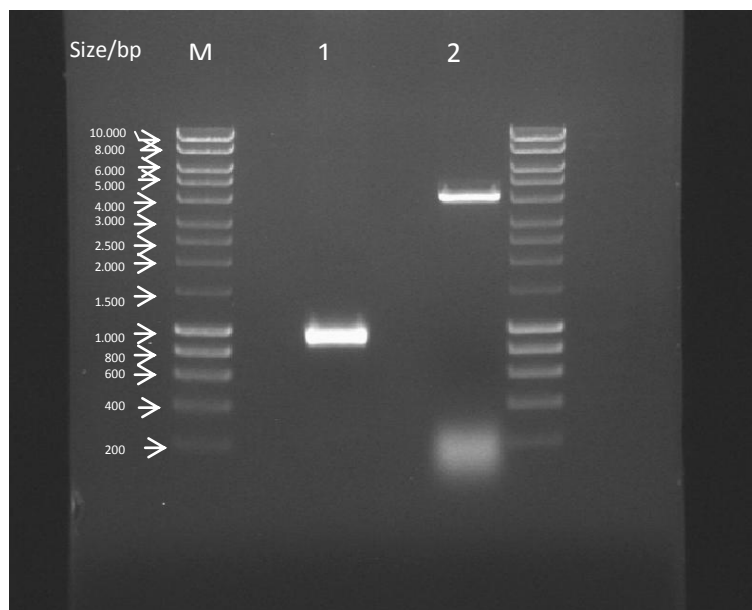
Figure 12. Mouse *Nanog* and pCS2+ double digested with Bam HI and Xho I

M, Hyperladder I. 1, Mouse *Nanog* cDNA double digested with Bam HI and Xho I. 2, pCS2+ double digested with Bam HI and Xho I . In lane 1 is a band of about 900 bp. It is mouse *Nanog* double digested with Bam HI and Xho I. In lane 2 are two bands, the bright single band of about 4,000 bp and the smear of approximately 200 bp, which is expected for the complete double digestion of pCS2+ by Bam HI and Xho I.

Figure 13. mnanog-pCS2+ 1-5 double digested with EcoR I and Xho I

M, Hyperladder I. 1-5, mnanog-pCS2+ constructs 1-5 double digested with EcoR I and Xho I. In lanes 1-5 are bands of mnanog-pCS2+ constructs 1-5 double digested with EcoR I and Xho I. Bands in all these lanes have the same pattern except those in lane 3. There are three bands in lanes 1, 2, 4 and 5. The size of two of them is about 850 bp and 4,000 bp, which is expected for double digestion products of mnanog-pCS2+ by EcoR I and Xho I and confirms that mnanog-pCS+ constructs 1,2,4 and 5 have inserts. The other band of about 5,000 bp probably represents uncut mnanog-pCS2+, which results from incomplete digestion reaction. In lane 3 there are four bands, including two expected bands of about 850 bp and 4,000 bp and the other two of about 5,000 bp and 7,500 bp, which probably owes to incomplete digestion.
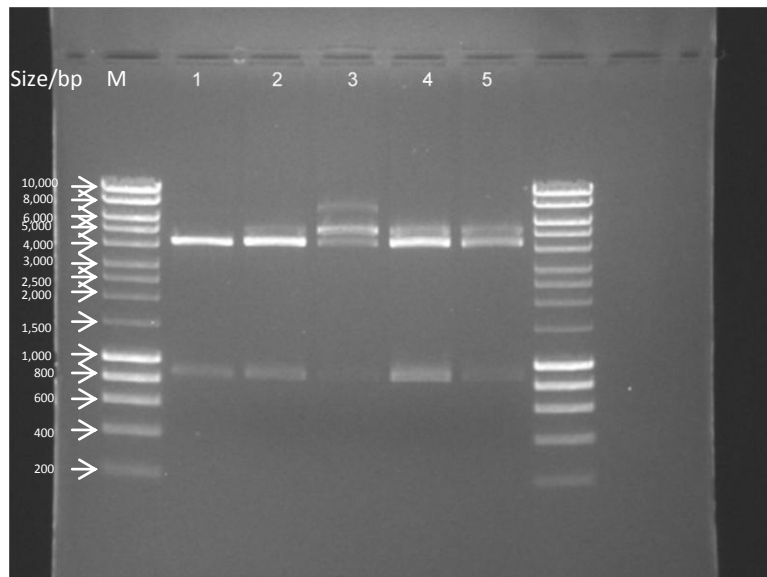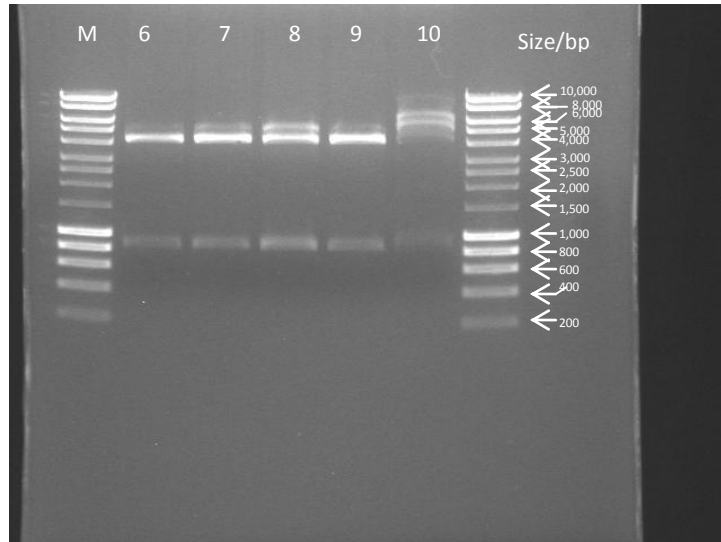
Figure 14. mnanog-pCS2+ 6-10 double digested with EcoR I and Xho I

M, Marker Hyperladder I. 6-10, mnanog-pCS2+ 6-10 double digested with EcoR I and Xho I. In lanes 6-10 are bands of double digestion of mnanog-pCS2+ 6-10 with EcoR I and Xho I. In lanes 6-9 digested mnanog-pCS2+ share the same band pattern with digested mnanog-pCS2+ 1, 2, 4 and 5 (Figure 13), three bands located at positions of 0.85 kb, 4 kb and 5 kb. In lane 10, there are five bands, two of which, of approximately 0.85 kb and 4 kb, are expected products of double digestion and the other three, of about 5 kb, 6.5 kb and 9 kb, are probably caused by incomplete digestion.
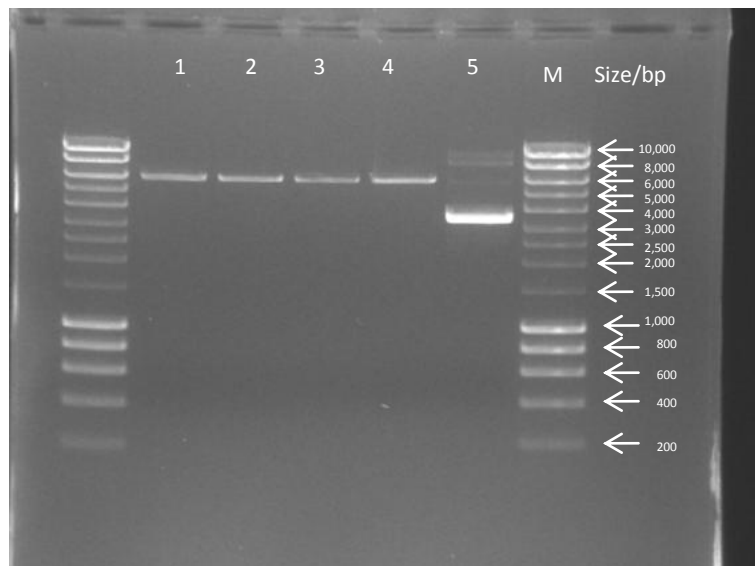
Figure 15. mnanog-pCS2+ ASP718

M, Marker Hyperladder I. 1-4: linearized mnanog-pCS2+. 5, uncut mnanog-pCS2+. In lanes 1-4 are the linearized mnanog-pCS2+ product which is a neat single band, demonstrating complete digestion compared with the bands of uncut mnanog-pCS2+ in lane 5.
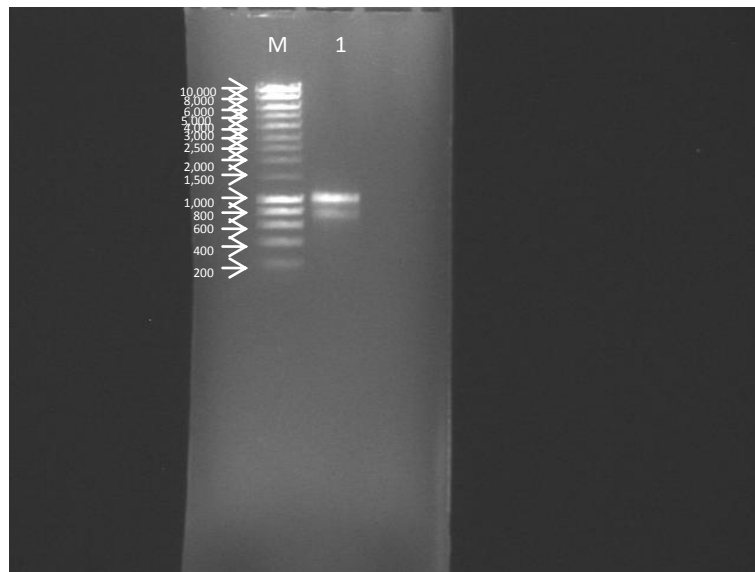
Figure 16. Mouse *Nanog* mRNA

M, Marker Hyperladder I. 1,Mouse *Nanog* mRNA. In lane one are bands of mouse *Nanog* mRNA. There are two bands, one of about 0.8 kb and the other of about 1 kb. The band pattern represents distribution of RNA conformations.

CHAPTER 3 *NANOG* overexpression does not affect the number of PGCs but affects dorsoventral patterning

3.1 Introduction

Nanog is expressed in mouse germ cells during the period of epigenetic erasure and germ line commitment (Yamaguchi et al., 2005) and is thought to mediate germline development (Chambers et al., 2007). It is essential for PGCs to complete colonizing the genital ridge (Chambers et al., 2007). Embryonic stem cells with *Nanog* disrupted can contribute to the germ line but *Nanog*-deficient primordial germ cells stay in the soma rather than reaching the genital ridge beyond the E11.5 stage (Chambers et al., 2007). So we hypothesize that it has an equivalent function in zebrafish germline development. In order to address this question, we misexpressed human *NANOG* and mouse *Nanog* mRNA in zebrafish embryos. We used mouse *Nanog* and human *NANOG* in this project because no clear orthologue of *Nanog* in zebrafish was apparent at the time. Although a *Nanog* homolog has been cloned from medaka recently and a putative zebrafish *nanog* has been identified, the degree of the similarity is overall very low compared with human *NANOG* and mouse *Nanog* (Camp et al., 2009). Nevertheless, functional studies with the putative zebrafish *nanog* are warranted, such as gain-of-function overexpression and loss-of-function knockdown with morpholinos. In zebrafish, *vasa* RNA and *nanos* RNA are components of germ plasm and markers of primordial germ cells (Yoon et al., 1997; Braat et al., 1999; Köprunner et al., 2001). Therefore we used *nanos* probe to detect primordial germ cells in embryos injected with human *NANOG* mRNA and in uninjected control embryos. We find that *NANOG*

overexpression does not affect the number of PGCs. Overexpression of either human *NANOG* or mouse *Nanog*, however, leads to dorsalized changes in the morphology of zebrafish embryos and suggests defects in dorsoventral patterning.

3.2 Materials

Special Equipment

Needle pippet puller	KOPF
Glass capillaries with inner filament	WPI
Microloader	Eppendorf
Microscope	Leica
Microscope	ZEISS

Chemicals

2% phenol red

mineral oil

human *NANOG* and mouse *Nanog* mRNA (kept at -80 degree)

nanos probe (obtained from Kong Jun)

Tricaine (MS-222)

3.3 Methods

Microinjection and whole mount in situ

Wild-type zebrafish embryos were collected and injected at the one-cell or two-cell stage with four sets of *NANOG/Nanog* mRNA, 50 pg human *NANOG* mRNA, 100 pg human *NANOG* mRNA, 50 pg mouse *Nanog* mRNA and 100 pg mouse *Nanog* mRNA on the same day. Injection of 50 pg and 100 pg mouse *Nanog* was repeated once on another day. Injection of 50 pg and 100 pg human *NANOG* was repeated for four times on four other days (one set of 50 pg human *NANOG* and one set of 100 pg human *NANOG* injected on one day). Embryos injected with *NANOG/Nanog* mRNA were classified into groups according to their morphology and counted. They were anesthetised with tricaine (0.016%) for photograph.

Whole mount in situ hybridisation with *nanos* probe was performed to detect the presence of primordial germ cells (Köprunner et al., 2001). In situ hybridization was performed according to the standard protocol (Thisse et al., 1993). The number of stained primordial germ cells was counted under microscope.

T-tests

As the number of PGCs is independent in *NANOG*-injected and uninjected control embryos and is normally distributed, we performed a two-tailed t-test with two samples assuming unequal variances to compare the number of PGCs in *NANOG*-injected and uninjected control embryos. In this chapter, a difference with p value smaller than 0.05 was considered significant.

3.4 Results

3.4.1 Germ line development

Number of primordial germ cells

Embryos injected with 100pg human *NANOG* could be classified into three categories according to their phenotype at 26-somite stage, truncated tail, split axes and normal (Figure 17a and 17b). As discussed by Köprunner et al. (2001), *nanos*-expressing cells are primordial germ cells. In order to assess the effects of overexpression of human *NANOG* mRNA on zebrafish germ line development, the number of primordial germ cells in three categories of *NANOG*-injected embryos was counted compared with the number of PGCs in uninjected control embryos (Figure 17a and 17b; Figure 18a and 18b; Table 1; Figure 19).

T-tests

Results of t-tests with two samples assuming unequal variances show that p values of all the comparisons in the number of PGCs (*NANOG*-injected embryos with normal phenotype vs uninjected control embryos, *NANOG*-injected embryos with split axes vs uninjected control embryos, and *NANOG*-injected embryos with truncated phenotype vs uninjected control embryos) are bigger than 0.05 (Table 2), indicating that the number of primordial germ cells doesn't change significantly in *NANOG*-injected embryos compared with that in uninjected control embryos.

a

Lateral views   Dorsal views

Truncated

A   p   A   p

Split axes

A   P   A   p

Normal

A   P   A   P
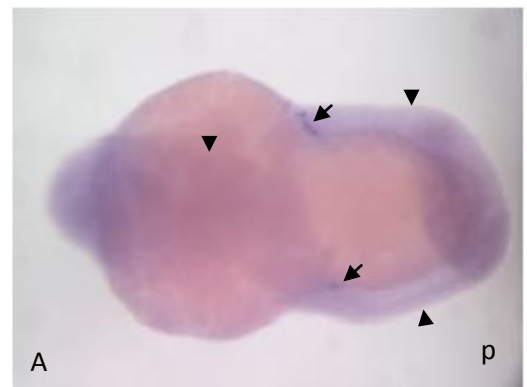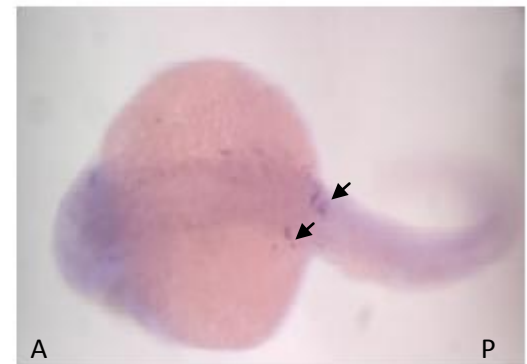
b
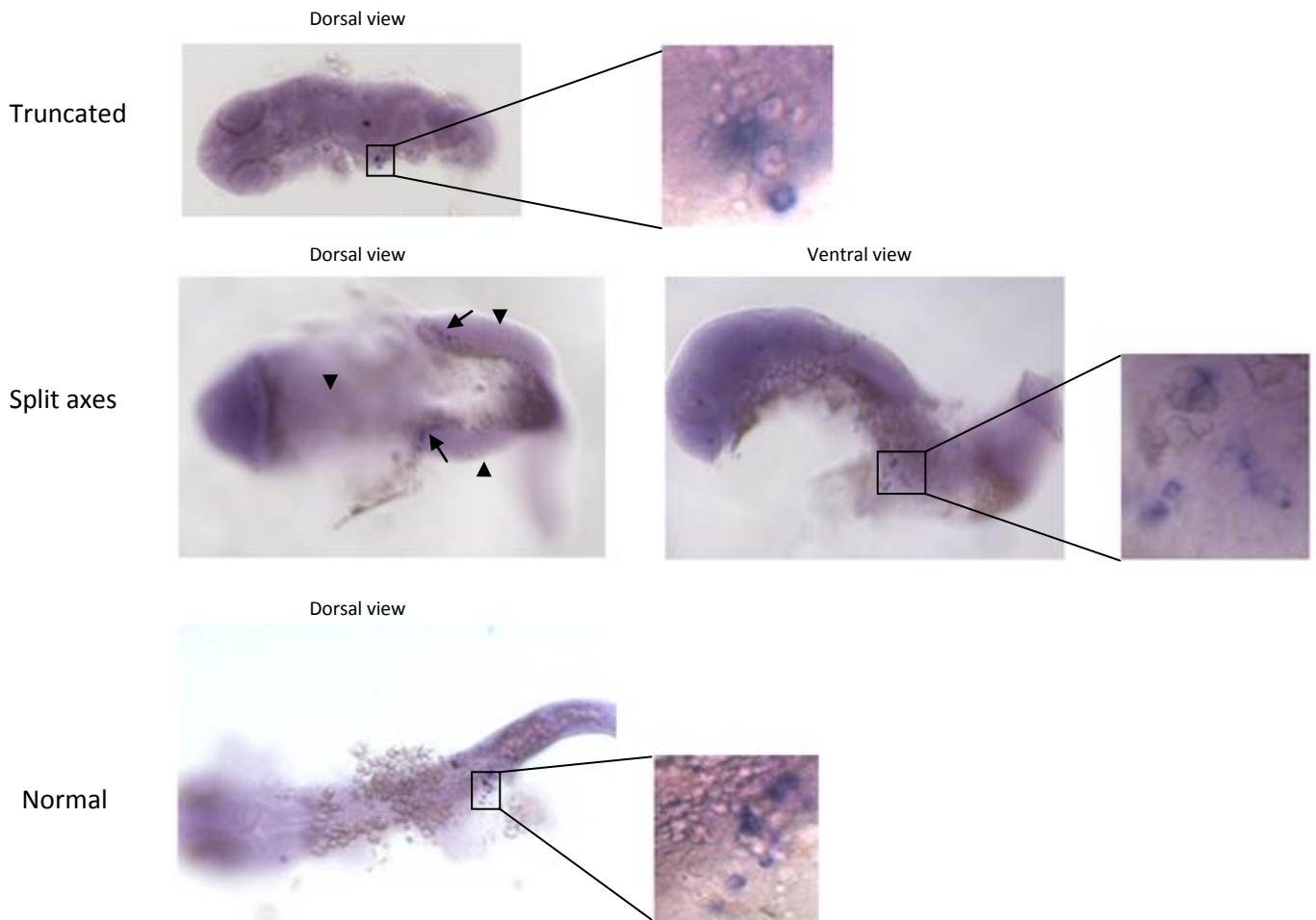
Figure 17. Whole mount in situ of *nanos* at 26-somite stage in embryos injected with 100 pg human *NANOG* mRNA. a, lateral views and dorsal views of *in situ* embryos. b, flattened embryos with yolks removed. In rectangulars are primordial germ cells. Arrows point to primordial germ cells. Arrowheads point to axes.

a
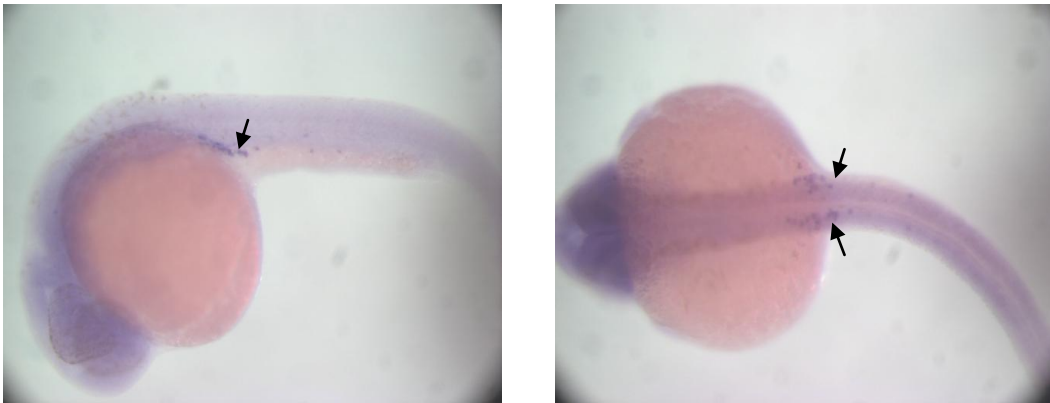
b
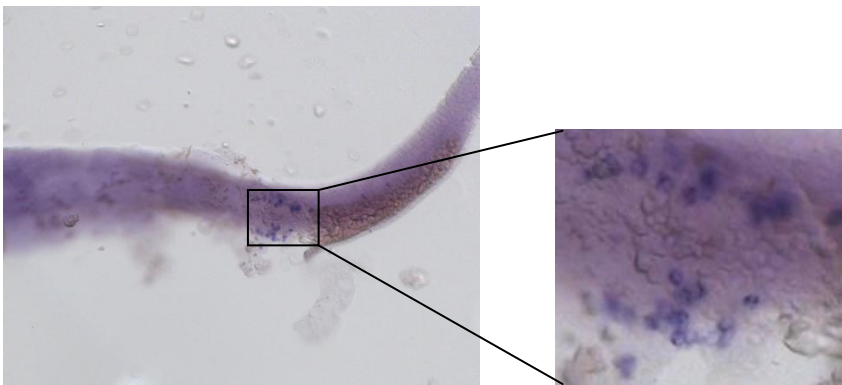
Figure 18. Whole mount in situ of *nanos* at 26-somite stage in uninjected control embryos.

a, a lateral view and a dorsal view of an *in situ* embryo. Arrows point to primordial germ

cells. b, a flattened embryo with the yolk removed. In the rectangular are primordial germ

cells.

Table 1. Number of primordial germ cells in *NANOG*-injected embryos and uninjected control embryos

	Number of primordial germ cells in each embryo for two independent injections	Mean	Standard Deviation	Morphology
Human *NANOG* 100 pg	12,15	13.5	2.1	Truncated
	10,8,12,15,11,6,8,10,9,16,21,22,12	12.3	4.9	Split axes
	14,15,12,7,14,17	13.2	3.4	Normal
Uninjected	15,17,15,13	15	1.6	Normal
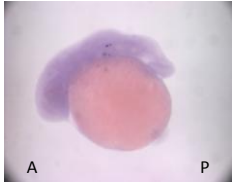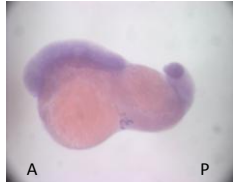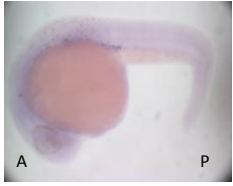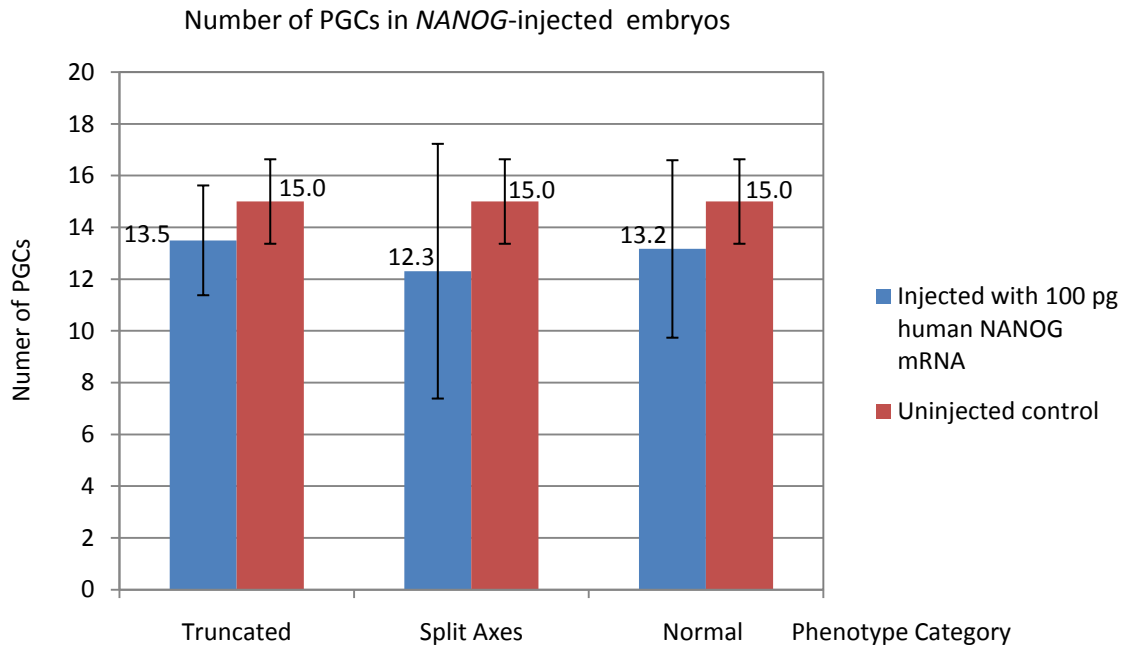
Figure 19. Number of PGCs in *NANOG*-injected embryos compared with uninjected control embryos

Table 2. p values of rejecting significant changes in the number of PGCs in three categories of *NANOG*-injected embryos according to their phenotype

	p value
NANOG-injected embryos with truncated-tail phenotype vs uninjected control embryos	0.489747
NANOG-injected embryos with split axes vs uninjected control embryos	0.111738
NANOG-injected embryos with normal phenotype vs uninjected control embryos	0.292814

3.4.2 Dorsoventral patterning

We next tested the effects of mouse *Nanog* and human *NANOG* on zebrafish development. Morphology of zebrafish embryos injected with human *NANOG* mRNA and mouse *Nanog* mRNA was recorded (Figure 20a and 20b). There are four categories of phenotype at 26-somite stage, truncated tails (truncated), split axes in the posterior trunk (split axes), abnormal tail and normal (Figure 20a and 20b). It suggests that overexpression of human *NANOG* mRNA or mouse *Nanog* mRNA causes a defect in dorsoventral patterning. Table 3 illustrates the dorsalized changes in the morphology of zebrafish embryos injected with 50 pg and 100 pg human *NANOG* and mouse *Nanog* mRNA and their number. There is a clear concentration-dependent effect with higher doses giving severer truncations and split axes. Among the sixty nine embryos injected with 50 pg human *NANOG* mRNA, 25% are with abnormal tail and 75% are with normal phenotype. The total percentage of abnormal embryos rose up to 56% when we increased the dose of human *NANOG* mRNA up to 100 pg. 18% of embryos are with truncated tails and 38% are with split axes. Among the sixteen embryos injected with 50 pg mouse *Nanog* mRNA, 81% are with split axes and 19% are with normal phenotype. When the dose rises up to 100pg, there are 23% of embryos with truncated phenotype, 10% with split axes and 49% with abnormal tails.

a

Truncated

Split axes

Abnormal tail

Normal

b
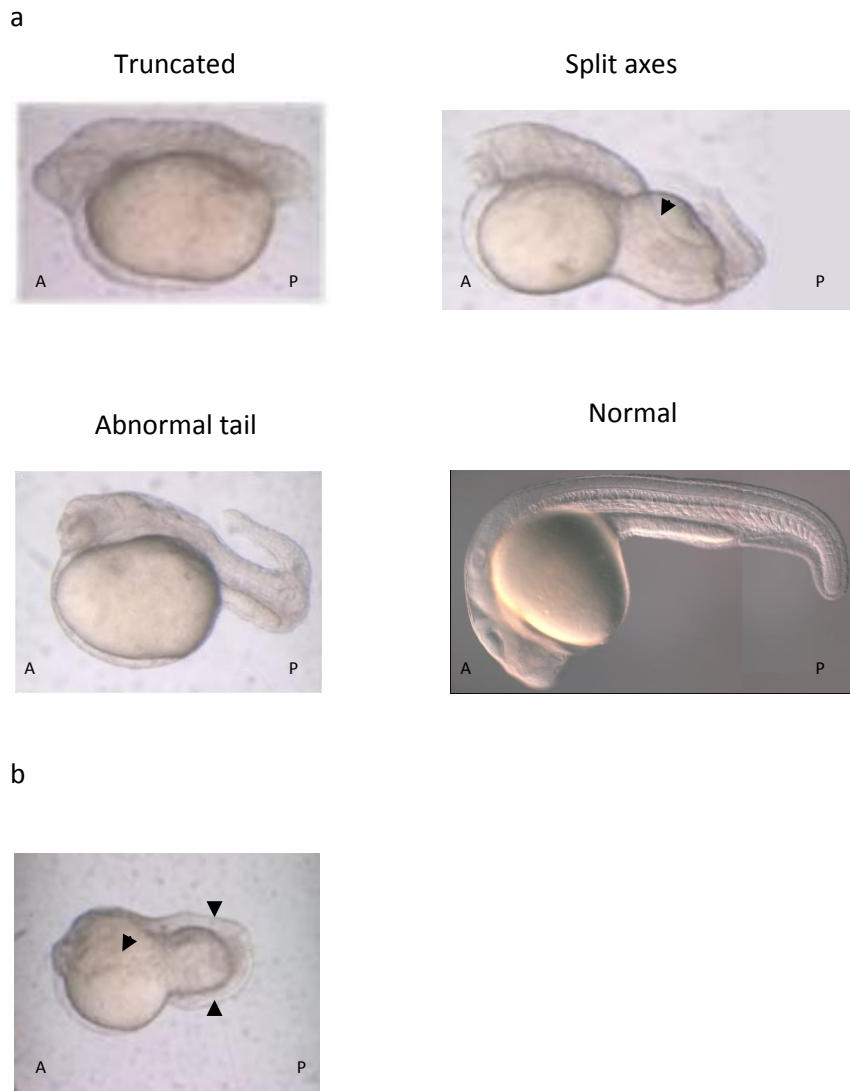
Figure 20. Zebrafish embryos injected with human *NANOG* or mouse *Nanog* mRNA at 26-somite stage.   a, phenotypes of *NANOG*-injected or *Nanog*-injected embryos at 26-somite stage. b, a dorsal view of an embryo with split axes at 26-somite stage. Arrowheads point to axes.

Table 3. Changes in morphology of zebrafish embryos after injection of *NANOG*/*Nanog*

Morphology	Truncated	Split Axes	Abnormal tail	Normal	Total Number
Human *NANOG* 50pg	--	--	17	52	69
Human *NANOG* 100pg	7	--	15	17	39
Mouse *Nanog* 50pg	--	13	--	3	16
Mouse *Nanog* 100pg	9	4	19	7	39

CHAPTER 4 Overexpression of mammalian *NANOG/Nanog* hyperdosalises zebrafish embryos

4.1 Introduction

In chapter 3, the morphology of *NANOG/Nanog*-injected embryos suggests a defect in dorsal-ventral patterning (Driever, 1995). Therefore we hypothesize that overexpression of *NANOG/Nanog* would alter expression of some dorsal-ventral genes but we are uncertain about whose expression it would affect (Schier and Talbot, 2005). In order to further investigate the effects of *NANOG/Nanog* on zebrafish dorsoventral patterning, we evaluated the specific effects of *NANOG/Nanog* on expression of three dorsal genes *chordin*, *squint* and *goosecoid* (Stachel et al., 1993; Schulte-Merker et al., 1994; Schulte-Merker et al., 1997; Dougan et al., 2003), and two ventral genes *wnt8a* and *bmp2b* (Kishimoto et al., 1997; Nguyen et al.,1998; Lekven et al., 2001; Ramel and Lekven, 2004) in this chapter. Quantitative RT-PCR has been an efficient method to assess gene expression at transcript levels and therefore was utilized to evaluate whether overexpression of *NANOG/Nanog* significantly changed expression of these five dorsal-ventral genes (Freeman et al., 1999). Simultaneous amplification of reference genes is a common method for normalising quantitative RT-PCR data (Bustin, 2000; Vandesomplete et al., 2002). In zebrafish, *beta-actin* is one of the commonly used normalisers for quantitative RT-PCR (Tang et al., 2007). It is stably expressed in the first few days of zebrafish development and is expressed in most tissues (Tang et al., 2007). It is suitable for zebrafish developmental time course analysis and is stably expressed following experimental manipulation (Tang et al., 2007; McCurley and

Gallard, 2008). Therefore in this chapter it was used to normalise variances in gene expression caused by amount and quality of different samples. We find that overexpression of *NANOG/Nanog* significantly upregulates expression of the dorsal gene *goosecoid* and significangly downregulates expression of the ventral gene *wnt8a,* which is consistent with the dorsalized phenotypes in mammalian *NANOG*/*Nanog*-injected embryos in chapter 3.

4.2 Materials

Special Equipment

NanoDrop	ND-1000 Spectrophotomer
Micropipet puller	KOPF
Glass capillaries with inner filament	WPI
Microloader	Eppendorf
Electrocoating bath	Apollo Instrumentation
Peltier Thermal Cycler	MJ Research
Real-time PCR thermal cycler	

Kits, enzymes and chemicals

KOD Hot Start PCR Kit (Novagen)

Ultra Pure^{TM} Agarose (Invitrogen)

DNA marker HyperLadder I and HyperLadder IV (Bioline)

Ethidium bromide   10 mg/ml (Sigma)

SuperScriptII Reverse Transcriptase

DNase I (RNase-free).

Human *NANOG* and mouse *Nanog* mRNA (kept at -80 degree)

5X First strand buffer

10X DNase Buffer

2X Taqman mix

TRIZOL

Isopropanol

70% ethanol

Phenol:Chloroform:isoamyl alcohol

DTT

beta-actin primers

beta-actin taqman probe

chordin taqman probe

squint taqman probe

goosecoid taqman probe

wnt8a taqman probe

bmp2b taqman probe

2% phenol red

mineral oil

4.3 Methods

Microinjection of human *NANOG* and mouse *Nanog*

H725 fish were set up the night before injection. Embryos were collected the next day. Two sets of *NANOG/Nanog* mRNA, 100 pg human *NANOG* mRNA and 100 pg mouse *Nanog* mRNA was injected into embryos at one-cell or two-cell stage on the same day. Twenty embryos injected with *NANOG/Nanog* mRNA were later collected at shield stage and pooled together as one biological replicate. We collected three replicates in total for human *NANOG* mRNA and mouse *Nanog* mRNA each. Another three biological replicates, each with twenty uninjected embryos pooled together in the same way, were used as control.

Total RNA isolation and reverse transcription

The embryos pooled together were frozen on dry ice. Total RNA was isolated from embryos following a standard protocol (Materials and Methods Appendix). Reverse transcription was performed and cDNA was made (Materials and Methods Appendix).

Quantitative RT-PCR

Quantitative RT-PCR is used to quantify expression of five genes, *chordin*, *squint*, *goosecoid*, *wnt8a* and *bmp2b*. Ct is the cycle number required for specific DNA to reach a threshold of amplification, which is detected by fluorescence its taqman probe generates. The more cycles required to reached the threshold means the less the quantity of specific DNA in the initial sample for amplification. Log 10 of the initial concentration of specific DNA in known samples against Ct generates a straight line, which is standard curve (Higuchi et al., 1993). It enables us to assess the quantity of specific DNA in unknown samples. In order to assess the quantities of *chordin*, *sqt*, *goosecoid*, *wnt8a*, *bmp2b* and *beta-actin*, standard curves of *chordin*, *squint*, *goosecoid*, *wnt 8a*, *bmp2b* and *beta-actin* were yielded with linear regression of a plot of log 10 of their quantities against Ct in a series of diluted cDNA mix (undiluted, 1 in4, 1 in 16, 1 in 64, 1 in 256, and 1 in 1024) of three uninjected control replicates. The standard curves were then used to evaluate the quantities of transcripts in total cDNAs of *NANOG/Nanog*-injected replicates and uninjected control replicates. The quantity of *beta-actin* here was used to normalize variances caused by amount and quality of different samples.

T-tests

We aimed to compare mean of normalized quantities of *chordin*, *squint*, *goosecoid*, *wnt8a* and *bmp2b* in cDNA replicates from *NANOG/Nanog*-injected embryos and uninjected control embryos. As the two samples are independent and transcript levels of these genes are normally distributed in *NANOG/Nanog*-njected embryos and uninjected control embryos, we performed a two-tailed t-test with two samples assuming unequal variances to test the difference. Difference in normalized quantities with p value smaller than 0.1 was considered significant in this chapter.

4.3 Results

Total RNA extraction and reverse transcription

Gel electrophoresis of RNA shows that RNA of good quality was obtained, with two bands of about 750 bp and 1,300 bp, representing distribution of RNA conformations (Figure 21). Figure 22 illustrates PCR amplification of *beta-actin* segments from cDNAs of three *NANOG*-injected replicates, three *Nanog*-injected replicates and three uninjected control replicates. The 400 bp *beta-actin* segment can be amplified from all the cDNAs, which indicates that the cDNAs are of good quality and could be used for quantitative RT-PCR assays. All bands are of similar brightness, indicating that *beta-actin* in all the cDNAs are of similar quantity.
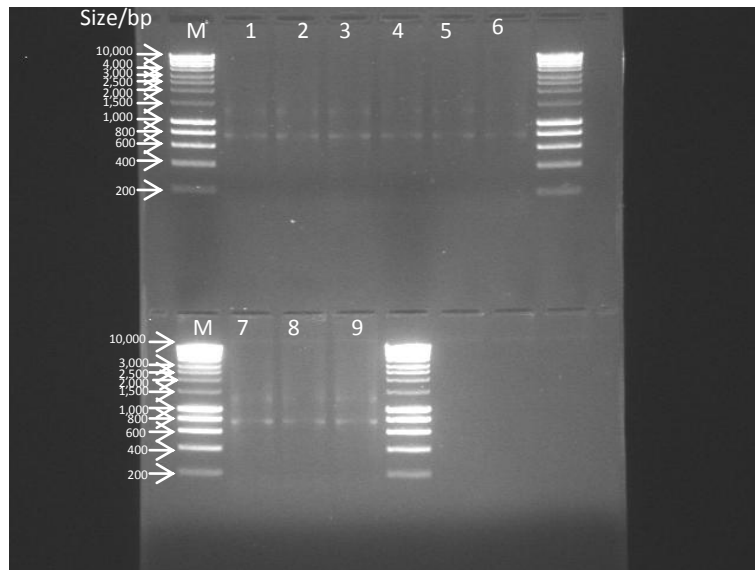
Figure 21. RNA Gel Electrophoresis

1-3, RNA extracted from three replicates of embryos injected with 100 pg human *NANOG*. 4-6, RNA extracted from three replicates of embryos injected with 100 pg mouse *Nanog*. 7-9, RNA extracted from three replicates of uninjected control embryos. M, Marker Hyperladder I. Band pattern of all the nine lanes is the same. There are two bands in each lane, of approximately 750 bp and 1,300 bp. These bands represent distribution of RNA conformation.
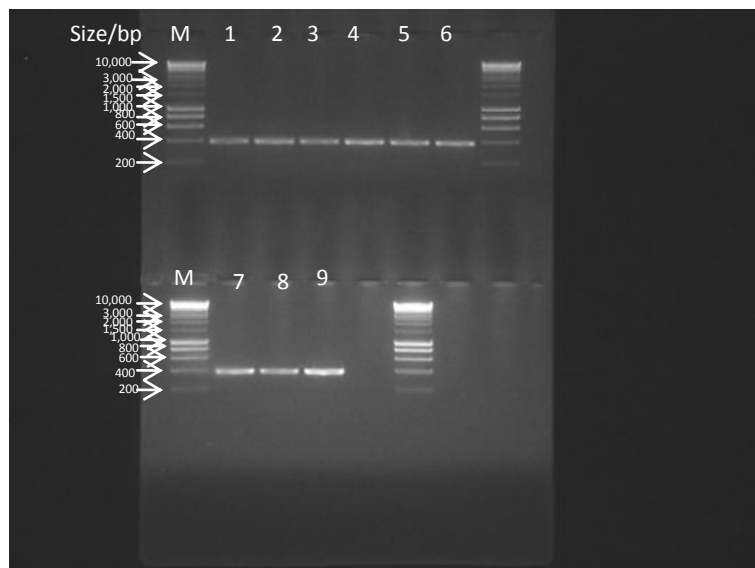
Figure 22. PCR amplification of the *beta-actin* segment

In lanes 1-9 are *beta-actin* segments amplified from cDNAs of nine samples (1-3, three replicates of embryos injected with 100 pg human *NANOG*; 4-6, three replicates of embryos injected with 100 pg mouse *Nanog*; 7-9, three replicates of uninjected control embryos). M, Marker Hyperladder I. There is a clear single band of about 400 bp in each lane.

Quantitative RT-PCR

Quantitative RT-PCR is an effective way of quantifying gene expression (Freeman et al., 1999). The work described in this session is aimed to quantify expression of five genes *chordin*, *squint*, *goosecoid*, *wnt8a,* and *bmp2b* in *NANOG*-injected embryos, *Nanog*-injected embryos and uninjected control embryos. Standard curves are generated by plotting log 10 of the initial quantities of these five genes and *beta-actin* against their cycle numbers (Ct) at which amplification detected by fluorescence from their samples reaches the threshold in a series of diluted cDNA mix (undiluted, 1 in4, 1 in 16, 1 in 64, 1 in 256 and 1 in1024) of uninjected replicates (Results Appendix). Log 10 of quantities of *chordin*, *squint, goosecoid*, *wnt8a*, *bmp2b* and *beta-actin* in *NANOG/Nanog*-injected and uninjected replicates are then inferred from standard curves with their cycle numbers used to reach the threshold of amplification (Results Appendix). Therefore expression of *chordin*, *squint*, *goosecoid*, *wnt8a,* and *bmp2b* in *NANOG/Nanog*-injected replicates and uninjected control replicates can be quantitatively measured by normalizing their quantities with quantities of *beta-actin*. Figure 23 illustrates quantities of *chordin*, *squint*, *goosecoid*, *wnt8a,* and *bmp2b* relative to quantities of *bactin*.
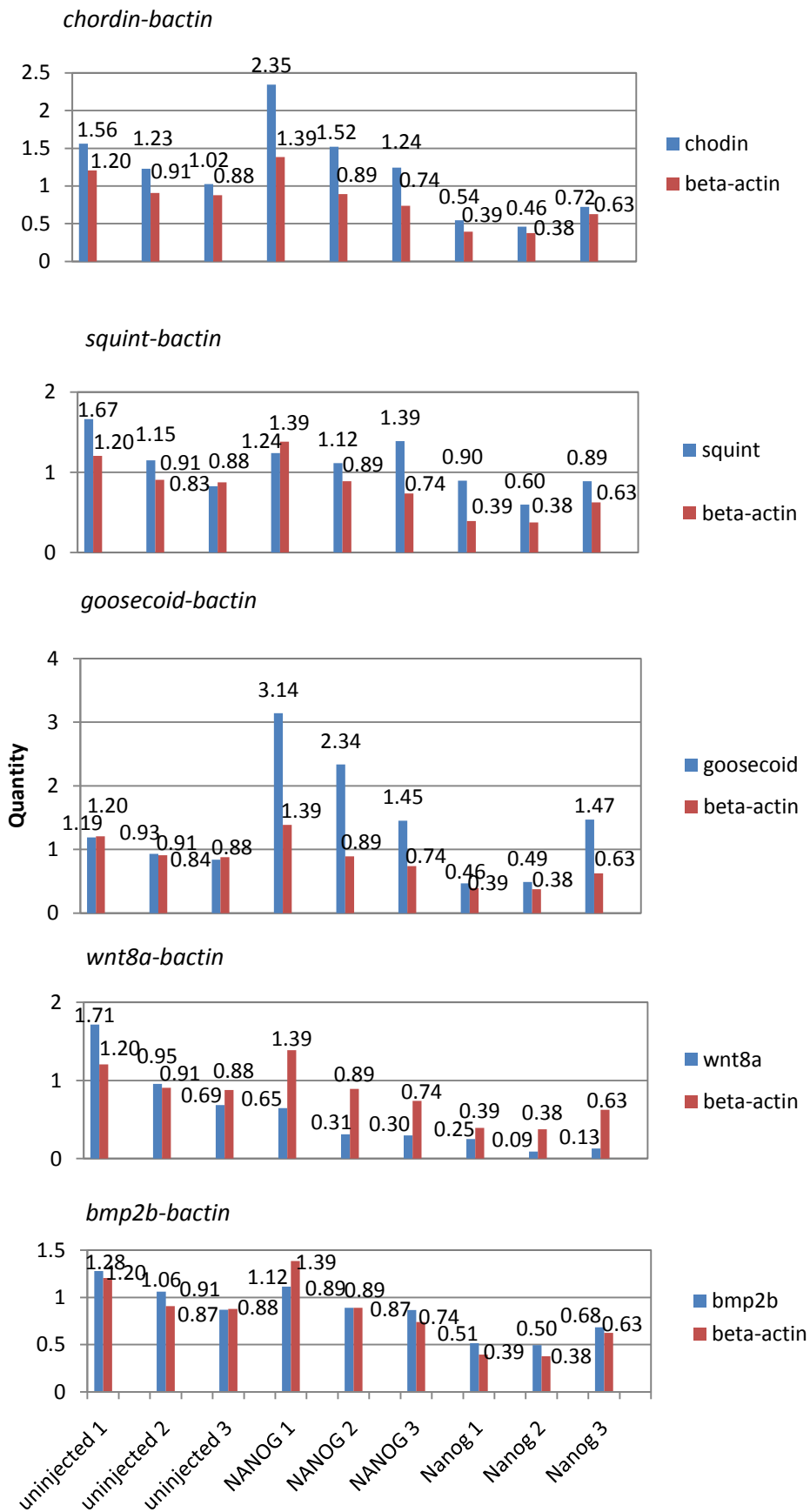
Figure 23. Quantities of *chd, sqt, gsc, wnt8a* and *bmp2b* relative to *bactin*

Figure 23. Quantities of *chd*, *sqt*, *gsc*, *wnt8a* and *bmp2b* relative to *beta-actin*. Three replicates of uninjected embryos are labelled uninjected 1, uninjected 2 and uninjected 3 in the horizontal axis. In a similar way, three replicates of embryos injected with human *NANOG* are labelled as *NANOG* 1-3. Three replicates of embryos injected with mouse *Nanog* are labelled as *Nanog* 1-3.

T-tests

T-tests were performed to test whether injection of mammalian *NANOG/Nanog* mRNA causes significant changes in gene expression of *chordin*, *squint*, *goosecoid*, *wnt8a* and *bmp2b* (p values are shown in table 4). The results show that overexpression of *NANOG/Nanog* significantly upregulates expression of the dorsal gene *goosecoid*, and significantly downregulates expression of the ventral gene *wnt8a* (Figure 24; Table 4). This is consistent with the dorsalized phenotypes of *NANOG/Nanog*-injected embryos.

Table 4. p values of rejecting significant difference in five genes' expression between *NANOG/Nanog*-injected and uninjected embryos

Comparison in gene expression between *NANOG/Nanog*-injected and uninjected embryos	p value
chordin	0.128799
squint	0.177210
goosecoid	0.009049
wnt8a	0.070615
bmp2b	0.666329
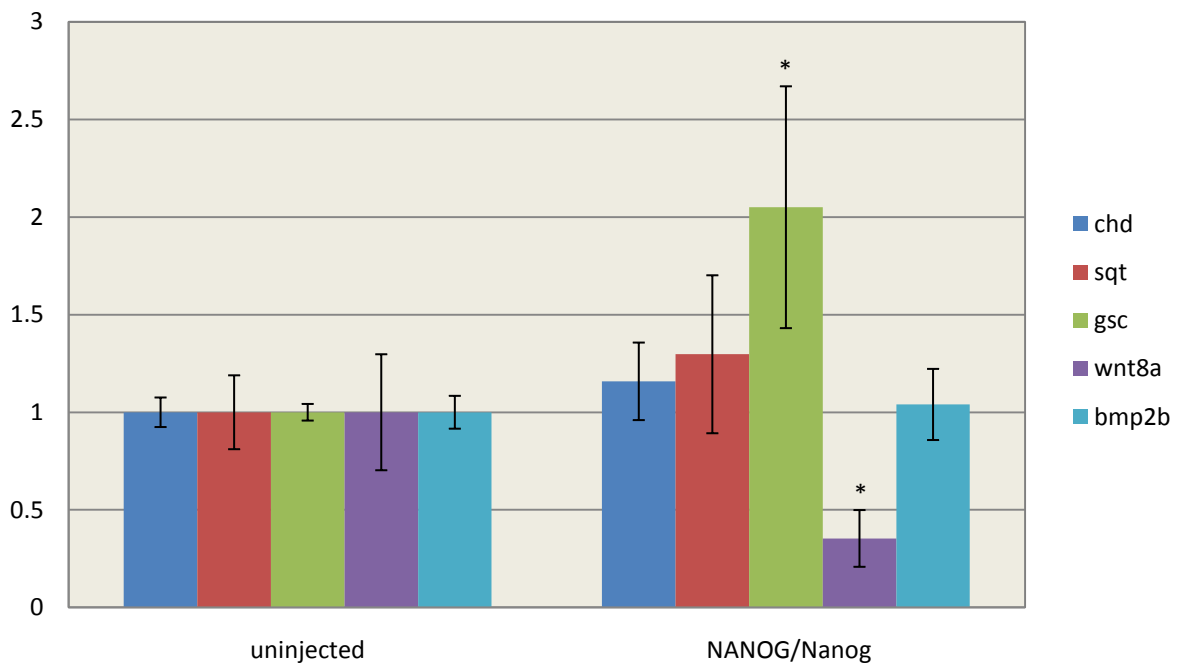
Figure 24. Bar chart showing the changes in expression of five dorsal and ventral genes after injection with *NANOG/Nanog* mRNA. Expression of *goosecoid* is significantly upregulated, while *wnt8a* expression is significantly downregulated. Upregulation of *goosecoid* expression and downregulation of *wnt8a* expression are labelled with * in the chart. The change would be rejected with p value smaller than 0.1 for them. Expression of *chordin*, *squint* and *bmp2b* are not significantly altered in injected embryos.

Chapter 5 Conclusions

Nanog has been found to be essential in promoting mouse germ line development (Chambers et al., 2007). In order to investigate whether it impacts zebrafish germ line development, we overexpressed mammalian *NANOG/Nanog* mRNA in zebrafish (Chambers et al., 2003; Mitsui et al., 2003). Human *NANOG* and mouse *Nanog* were used in this thesis because when we started there was no clear orthologue of human *NANOG* or mouse *Nanog* in zebrafish. We find that *NANOG* overexpression in zebrafish embryos doesn't change the number of primordial germ cells but affects dorsoventral patterning. The work presented in this thesis shows the first investigation of microinjecting mammalian *NANOG/Nanog* mRNA into zebrafish embryos, studying the effects of overexpressing mammalian *NANOG/Nanog* mRNA in zebrafish embryos on germ line development and dorsal-ventral patterning. The construction of hsnanog-pCS2+ and mnanog-pCS2+ and in vitro transcription of human *NANOG* and mouse *Nanog* mRNA have been presented in detail, followed by the discussion of dorsalized changes in the morphology of zebrafish embryos and no effect on the number of primordial germ cells after injection with *NANOG* mRNA. Quantitative RT-PCR (Freeman et al., 1999) was used to quantify expression of five genes involved in dorsal-ventral patterning, and t-tests were performed to investigate the changes in these genes' expression. It is found that overexpression of mammalian *NANOG/Nanog* mRNA significantly upregulates expression of the dorsal gene *goosecoid* (Stachel et al., 1993; Schulte-Merker et al., 1994) and significantly downregulates expression of the ventral gene *wnt8a* (Lekven et al.,

2001;Ramel and Lekven, 2004), which is consistent with the dorsalized phenotypes in *NANOG*/*Nanog*-injected embryos.

The investigation presented in this thesis contributes to our understanding of the effects of NANOG/Nanog on some zebrafish developmental features, and demonstrates that microinjection represents a valuable approach for studying *NANOG/Nanog* function. The results show that overexpression of mammalian *NANOG*/*Nanog* mRNA by microinjection leads to significant changes in the phenotype of the zebrafish embryos (25% and 56% of embryos show significant dorsalization in their phenotype after injection with 50pg and 100pg human *NANOG*; 81% and 82% of embryos show significant dorsalization in their phenotype after injection with 50pg and 100pg mouse *Nanog*), causing the mis-specification of fates along the dorsal-ventral axis, rather than verifying the original hypothesis that *NANOG* overexpression would lead to the overproduction of primordial germ cells in the zebrafish embryos (no significant change in the number of primordial germ cells can be observed following injection of human *NANOG* mRNA). However, previous studies in other model organisms such as mice show that *Nanog* is essential for specification of germ cells in their embryos (Chambers et al., 2007). There are three possible reasons that might lead to the difference between the experimental result and the original hypothesis: firstly, the transcription factor Nanog may function in different ways during the developmental processes of different model organisms (Chambers et al., 2007; Yamaguchi et al., 2009; Sánchez-Sánchez et al., 2010); Secondly, germ cells are specified by inheriting germ plasm in zebrafish (Raz, 2003), which is different from the way they are specified in mammals (Saga, 2008; Ewen and Koopman, 2010); thirdly, the difference between the technologies, such as exogenous induction, knockout and microinjection, that have been used in the experiments to study *Nanog* in the model organisms may lead to these different results (Chambers et al., 2003; Mitsui et al., 2003; Chambers et al., 2007; Yamaguchi et al., 2009) .

In order to further investigate the function of NANOG/Nanog, several approaches can be taken to supplement the current experiments or take the research a step further. One of them is to transfect dissociated zebrafish embryonic cells with *NANOG/Nanog* and score for *vasa* positive cells (Knaut et al., 2000). Another one is to inject the *piggyBAC* vector (Ding et al., 2005) carrying *NANOG/Nanog* gene into zebrafish embryos and score for *vasa* positive cells (Knaut et al., 2000). These two methods could be used to study whether *NANOG/Nanog* has an equivalent function in sustaining pluripotency as it does in human and mouse embryonic stem cells and the inner cell mass (Chambers et al., 2003; Mitsui et al.,2003; Chambers et al., 2007). However, these two methods are more time-consuming than microinjection. Also, more genes involved in dorsal-ventral patterning could be selected to investigate the function of NANOG/Nanog in the processes of zebrafish development. Moreover, only two sets of *NANOG/Nanog* mRNA injection dosage have been used in the current experiment because of the time constraint, more sets of injection dosage could be tested so that the effects of *NANOG/Nanog* overexpression might be further investigated. The estimation of gene expression is not ideal in this thesis because some of the data fall beyond the range of data points used for linear regression. Accuracy of the measurement could be improved by diluting cDNA samples of experimental replicates of embryos injected with human *NANOG* or mouse *Nanog* and control replicates of uninjected embryos.

The result that *NANOG* overexpression doesn't lead to a significant change in the number of primordial germ cells in zebrafish, supports the view that zebrafish animal cap, including somatic cells and primordial germ cells, doesn't develop from a pluripotent ground state. Frog, which has similar mechanism of primordial germ cell specification with zebrafish, doesn't have any *NANOG*/*Nanog* homologue in its genome (Hellsten et al., 2010). In contrast, Nanog has been identified as a regulator of pluripotency in many organisms

initiating somatic and germ cell development from ground state pluripotency, suggesting the conserved pluripotency network from urodele amphibians to mammals (Dixon et al., 2010).

As a homeodomain protein, NANOG/Nanog may function as a dominant negative form of Vox or Vent, suppressing function of Vox or Vent (Kawahara et al., 2000a; Kawahara et al., 2000b; Imai et al., 2001) and dorsalizing zebrafish embryos. To further investigate mechanism of NANOG/Nanog function, *vox* or *vent* RNA could be injected to test whether it could rescue the defect in dorsoventral patterning caused by *NANOG*/*Nanog* overexpression. RNA extracted from different stages of *NANOG*/*Nanog*-injected embryos could be sequenced to give a transcriptome view of the changes caused by *NANOG/Nanog* overexpression (Ryan et al., 2008; Wang et al., 2009). It could be compared with the transcriptome of zebrafish embryos injected with *vox* or *vent* dominant negative forms. Moreover, chromatin immunoprecipitation combined with sequencing could give information about NANOG/Nanog binding sites in zebrafish genome, which would be helpful for studying how NANOG/Nanog functions (Johnson et al., 2007; Jothi et al., 2008).

At the time we started the work, there was no clear orthologue of *Nanog* in zebrafish. A putative zebrafish *nanog* (Zgc: 193933) has been proposed recently (Camp et al., 2009). Similar approaches could be used to study the function of the potential zebrafish *nanog*. Zebrafish *nanog* mRNA could be overexpressed to study whether it has effect on the number of zebrafish PGCs and dorsoventral patterning.   On the other hand, it is also meaningful to introduce morpholinos of the putative zebrafish *nanog* to interrupt its endogenous expression for loss-of-function studies. According to the result of this thesis, no significant change in the number of zebrafish PGCs would be expected for gain-of-function or loss-of-function studies of zebrafish *nanog*. One possibility is that overexpressing zebrafish *nanog* would dorsalize embryos, while a morpholino knockdown would cause a ventralized phenotype.

However, a potential medaka *Nanog* has been identified, but its overexpression doesn't cause any specific change in phenotype (Camp et al., 2009), in contrast with the defect in dorsoventral patterning caused by overexpressing mammalian *NANOG*/*Nanog* in zebrafish described in this thesis. No effect of medaka *Nanog* overexpression might be attributed to the absence of WR domain in it, which mediates dimerization of mammalian NANOG/Nanog (Mullin et al., 2008; Wang et al., 2008). Therefore, mammalian NANOG/Nanog or medaka Nanog with WR domain inserted could be overexpressed in medaka to further these studies.

Follow-up studies on function of zebrafish *nanog* including rescue with *vox* or *vent* mRNA, RNA-seq (Ryan et al., 2008; Wang et al., 2009) and Chip-seq (Johnson et al., 2007; Jothi et al., 2008) could be used to investigate its interaction with other transcription factors as well as with zebrafish genome at different stages of zebrafish development.

As has been discussed in the previous chapters, several other transcription factors such as OCT4, SOX2, LIN28 and KLF4 appeal to researchers because of their special functionalities including promoting pluripotency (Yu et al., 2007). Further research using similar technologies as presented in this thesis could also be carried out to investigate the function of these important transcription factors in the developmental processes of zebrafish.

References

Alexander, T., Nolte, C. and Krumlauf, R. (2009). *Hox* genes and segmentation of the hindbrain and axial skeleton. *Annu Rev Cell Dev Biol*. **25**:431-456

Anderson, R., Fässler, R., Georges-Labouesse, E., Hynes, R.O., Bader, B.L., Kreidberg, J.A., Schaible, K., Heasman, J. and Wylie,C. (1999). Mouse primordial germ cells lacking beta1 integrins enter the germline but fail to migrate normally to the gonads. *Development* **126**(8):1655-1664.

Avilion, A.A., Nicolis, S.K., Pevny, L.H., Perez, L., Vivian, N. and Lovell-Badge, R. (2003). Multipotent cell lineages in early mouse development depend on SOX2 function. *Genes Dev.* **17**(1):126-140.

Bang, A.G., Papalopulu, N., Goulding, M.D. and Kintner, C. (1999). Expression of *Pax-3* in the lateral neural plate is dependent on a *Wnt*-mediated signal from posterior nonaxial mesoderm. *Dev Biol.* **212**(2):366-80

Bernex, F., De Sepulveda, P., Kress, C., Elbaz, C., Delouis, C. and Panthier, J.J. (1996). Spatial and temporal patterns of c-*kit*-expressing cells in $W^{lacZ/+}$ and W^{lacZ}/W^{lacZ} mouse embryos. *Development* **122**(10):3023-3033.

Blumberg, B., Wright, C.V.E., De Robertis, E.M. and Cho, K.W.Y. (1991). Organizer-specific homeobox genes in *Xenopus laevis* embryos. *Science* **253**(5016):194-196.

Braat, A.K., Zandbergen, T., van de Water, S., Goos, H.J. and Zivkovic, D. (1999). Characterization of zebrafish primordial germ cells: morphology and early distribution of *vasa* RNA. *Dev Dyn.* **216**(2):153-167.

Bustin, S.A. (2000). Absolute quantification of mRNA using real-time reverse transcription polymerase chain reaction assays. *J Mol Endocrinol* **25**: 169−193.

Camp, E, Sánchez-Sánchez, A.V., García-España, A., Desalle, R., Odqvist, L., Enrique O'Connor, J. and Mullor, J.L. (2009). Nanog regulates proliferation during early fish development. *Stem Cells.* **27**(9):2081-2091.

Chambers, I., Colby, D., Robertson, M., Nichols, J., Lee, S., Tweedie, S. and Smith, A. (2003). Functional expression cloning of Nanog, a pluripotency sustaining factor in embryonic stem cells. *Cell* **113**(5), 643-655.

Chambers, I., Silva, J, Colby, D, Nichols, J, Nijmeijer, B, Robertson, M, Vrana, J, Jones, K, Grotewold, L and Smith, A. (2007). Nanog safeguards pluripotency and mediates germline development. *Nature* **450**, 1230-1234.

Chambers, I. and Tomlinson, S.R. (2009)**.** The transcriptional foundation of pluripotency. *Development* **136**(14):2311-2322.

Chen,Y. and Schier, A.F. (2001). The zebrafish Nodal signal Squint functions as a morphogen. *Nature* **411**(6837):607-610.

Cho, K.W., Blumberg, B., Steinbeisser, H. and De Robertis, E.M. (1991). Molecular nature of Spemann's organizer: the role of the *Xenopus* homeobox gene *goosecoid. Cell* **67**(6):1111-1120.

Christian, J.L., McMahon, J.A., McMahon, A.P. and Moon, R.T. (1991). *Xwnt*-8, a Xenopus *Wnt*-1/*int*-1-related gene responsive to mesoderm-inducing growth factors, may play a role in ventral mesodermal patterning during embryogenesis. *Development* **111**(4):1045-1055.

Christian, J.L. and Moon, R.T. (1993) Interactions between *Xwnt*-8 and Spemann organizer signaling pathways generate dorsoventral pattern in the embryonic mesoderm of *Xenopus. Genes and Development* **7**:13-28.

Conlon, F.L., Lyons, K.M., Takaesu, N., Barth, K.S., Kispert, A., Herrmann, B. and Robertson, E.J. (1994). A primary requirement for *Nodal* in the formation and maintenance of the primitive streak in the mouse. *Development* **120**(7):1919-1928.

Dick, A., Hild, M., Bauer, H., Imai, Y., Maifel, H., Schier, A.F., Talbot, W.S., Bouwmeester,T. and Hammerschmidt, M. (2000). Essential role of *Bmp7* (*snailhouse*) and its prodomain in dorsoventral patterning of the zebrafish embryo. *Development* **127**(2): 343-354.

Ding, S., Wu, X., Li, G., Han, M., Zhuang, Y. and Xu, T. (2005). Efficient transposition of the *piggyBac* (*PB*) transposon in mammalian cells and mice. *Cell.* **122**(3):473-483.

Dixon, J.E., Allegrucci, C., Redwood, C., Kump, K., Bian, Y., Chatfield, J., Chen, Y.H., Sottile, V., Voss, S.R., Alberio, R. and Johnson, A.D. (2010). Axolotl *Nanog* activity in mouse embryonic stem cells demonstrates that ground state pluripotency is conserved from urodele amphibians to mammals. *Development* **137**(18):2973-2980.

Dougan,S.T., Warga, R.M., Kane, D.A., Schier, A.F. and Talbot, W.S. (2003). The role of the zebrafish *nodal*-related genes *squint* and *cyclops* in patterning of mesendoderm. *Development* **130**(9): 1837-1851.

Driever, W. (1995). Axis formation in zebrafish. *Curr.Opin.Genet.Dev.* **5**(5):610-618.

Erter, C.E., Solnica-Krezel, L. and Wright C.V.E. (1998). *Zebrafish nodal-related 2* encodes an early mesendodermal inducer signaling from the extraembryonic yolk syncytial layer. *Dev. Biol.* **204**(2):361-372.

Ewen, K.A. and Koopman, K. (2010). Mouse germ cell development: From specification to sex determination. *Molecular and Cellular Endocrinology* **323**: 76–93.

Feldman, B., Dougan, S.T., Schier, A.F. and Talbot, W.S. (2000). Nodal-related signals establish mesendodermal fate and trunk neural identity in zebrafish. *Curr Biol.* **10**(9):531-534.

Freeman, W.M., Walker, S.J., and Vrana, K.E. (1999). Quantitative RT-PCR: Pitfalls and Potential. *BioTechiniques* **26**: 112-125.

Frohnhöfer, H.G. and Nüsslein-Volhard, C. (1986). Organization of anterior pattern in the *Drosophila* embryo by the maternal gene *bicoid*. *Nature* **324**, 120-125.

Godin,I.,Wylie,C. and Heasman, J. (1990).Genital ridges exert long-range effects on mouse primordial germ cell numbers and direction of migration in culture. *Development* **108**,357-363.

Hammerschmidt, M., Pelegri, F., Mullins, M.C., Kane, D.A., van Eeden, F.J., Granato, M., Brand, M., Furutani-Seiki, M., Haffter, P., Heisenberg, C.P., Jiang, Y.J., Kelsh, R.N., Odenthal, J., Warga, R.M. and Nusslein-Volhard, C. (1996). *dino* and *mercedes*, two genes regulating dorsal development in the zebrafish embryo. *Development* **123**, 95–102.

Hanna, J.H., Saha, K, and Jaenisch, R. (2010). Pluripotency and cellular reprogramming: facts, hypotheses, unresolved issues.*Cell* **143**(4): 508-525.

Harvey, R.P. (1996)**.** *NK-2* homeobox genes and heart development, *Dev. Biol.* **178**: 203–216.

Heisenberg, C.P. and Nüsslein-Volhard, C. (1997). The function of *silberblick* in the positioning of the eye anlage in the zebrafish embryo. *Dev Biol.* **184**(1):85-94.

Hellsten, U., Harland, R. M., Gilchrist, M. J., Hendrix, D., Jurka, J., Kapitonov, V., Ovcharenko, I., Putnam, N. H., Shu, S., Taher, L. et al. (2010). The genome of the Western clawed frog *Xenopus tropicalis*. *Science* **328**, 633-636.

Higuchi, R., Fockler, C., Dolinger, G. and Watson. R. (1993). Kinetic PCR analysis: real-time monitoring of DNA amplification reactions. *Biotechnology* **11**(9):1026-1030.

Hill, R.E., Jones, P.F., Rees, A.R., Sime, C.M., Justice, M.J., Copeland, N.G., Jenkins, N.A., Graham, E. and Davidson, D.R. (1989). A new family of mouse homeobox-containing genes: molecular structure, chromosomal location, and developmental expression of *Hox-7.1*. *Genes Dev.* **3**(1):26-37.

Hsieh, J.C., Kodjabachian, L., Rebbert, M.L., Rattner, A., Smallwood, P.M., Samos, C.H., Nusse, R., Dawid, I.B., and Nathans, J. (1999). A new secreted protein that binds to Wnt proteins and inhibits their activities. *Nature* **398**, 431–436.

Hoppler, S., Brown, J.D. and Moon,R.T. (1996). Expression of a dominant-negative Wnt blocks induction of MyoD in *Xenopus* embryos. *Genes & Development* **10**: 2805-2817.

Houston, D.W. and King, M.L. (2000). Germ plasm and molecular determinants of germ cell fate. *Curr Top Dev Biol.* **50**:155-181.

Iimura, T., Denans, N. and Pourquié, O. (2009). Establishment of *Hox* vertebral identities in the embryonic spine precursors. *Curr Top Dev Biol.* **88**:201-234.

Ikenishi, K., Kotani, M. and Tanabe, K. (1974). Ultrastructural changes associated with UV irradiation in the "germinal plasm" of *Xenopus laevis*. **36**(1):155-168.

Imai, Y., Gates, M.A., Melby, A.E., Kimelman, D., Schier, A.F. and Talbot, W.S. (2001). The homeobox genes *vox* and *vent* are redundant repressors of dorsal fates in zebrafish. *Development* **128**, 2407-2420.

Johnson, A.D., Crother, B., White, M,E., Patient, R., Bachvarova, R.F., Drum, M. and Masi, T. (2003). Regulative germ cell specification in axolotl embryos: a primitive trait conserved in the mammalian lineage. *Philos Trans R Soc Lond B Biol Sci.* **358**(1436):1371-1379.

Johnson, D.S., Mortazavi, A., Myers, R.M. and Wold, B. (2007). Genome-wide mapping of *in vivo* protein-DNA interactions. *Science* **316**(5830):1497-1502.

Jones, C.M., Kuehn, M.R., Hogan, B.L.M., Smith, J.C. and Wright, C.V.E. (1995). Nodal-related signals induce axial mesoderm and dorsalize mesoderm during gastrulation. *Development* **121**(11):3651-3662.

Joseph, E.M. and Melton, D.A. (1997). *Xnr4*: a *Xenopus* nodal-related gene expressed in the Spemann organizer. *Dev. Biol.* **184**(2):367-372.

Jothi, R., Cuddapa, S., Barsk, A., Cui, K. and Zhao, K. (2008). Genome-wide identification of *in vivo* protein-DNA binding sites from ChIP-Seq data. *Nucleic Acids Res*. **36**(16):5221-5531.

Karin, M. (1990). Too many transcription factors: positive and negative interactions. *New Biol.* **2**(2):126-131.

Kawahara, A., Wilm, T., Solnica-Krezel, L. and Dawid, I.B. (2000a). Antagonistic role of *vega1* and *bozozok/dharma* homeobox genes in organizer formation. *Proc Natl Acad Sci* U S A. **97**(22):12121-12126.

Kawahara, A., Wilm, T., Solnica-Krezel, L. and Dawid, I.B. (2000b). Functional interaction of *vega2* and *goosecoid* homeobox genes in zebrafish. *Genesis* **28**, 58-67.

Kelly, G.M., Greenstein, P., Erezyilmaz, D.F. and Moon, R.T. (1995). Zebrafish *wnt8* and *wnt8b* share a common activity but are involved in distinct developmental pathways. *Development* **121**(6):1787-1799.

Kimmel, C.B., Ballard, W.W., Kimmel, S.R., Ullmann, B. and Schilling, T.F. (1995). Stages of embryonic development of the zebrafish. *Dev Dyn.* **203**(3):253-310.

Kim, Y. and Nirenberg, M. (1989). *Drosophila NK*-homeobox genes. *Proc Natl Acad Sci* U S A. **86**(20):7716-7720.

Kishimoto, Y., Lee, K.H., Zon, L., Hammerschmidt, M. and Schulte-Merker, S. (1997). The molecular nature of zebrafish *swirl*: BMP2 function is essential during early dorsoventral patterning. *Development* **22**, 4457-4466.

Knaut, H., Pelegri, F., Bohmann, K., Schwarz, H. and Nüsslein-Volhard, C. (2000). Zebrafish *vasa* RNA but not its protein is a component of the germ plasm and segregates asymmetrically before germline specification. *J Cell Biol.* **149**(4): 875–888.

Köprunner, M., Thisse, C., Thisse, B. and Raz, E. (2001). A zebrafish *nanos*-related gene is essential for the development of primordial germ cells. *Genes Dev.* **15**(21):2877-2285.

Krieg, P.A. and Melton, D.A. (1984). Functional messenger RNAs are produced by SP6 in vitro transcription of cloned cDNAs. *Nucleic Acids Res* **12**(18): 7057-7070.

Latchman, D.S. (1997). Transcription factors: an overview. *Int J Biochem Cell Biol.* **29**(12):1305-1312.

Lavial, F., Acloque, H., Bertocchini, F., Macleod, D.J., Boast, S., Bachelard, E., Montillet, G., Thenot, S., Sang, H.M., Stern, C.D., Samarut, J. and Pain, B. (2007). The Oct4 homologue PouV and Nanog regulate pluripotency in chicken embryonic stem cells. *Development* **134**(19):3549-3563.

Lawson, K.A., Dunn, N.R., Roelen, B.A., Zeinstra, L.M., Davis, A.M., Wright, C.V., Korving, J.P. and Hogan, B.L. (1999). *Bmp4* is required for the generation of primordial germ cells in the mouse embryo. *Genes Dev.* **13**(4):424-436.

Lekven, A.C., Thorpe, C.J., Waxman, J.S. and Moon, R.T. (2001). Zebrafish *wnt8* encodes two wnt8 proteins on a bicistronic transcript and is required for mesoderm and neurectoderm patterning. *Dev Cell.* **1**(1):103-114.

Liang, Z and Biggin, M.D. (1998). *Eve* and *ftz* regulate a wide array of genes in blastoderm embryos: the selector homeoproteins directly or indirectly regulate most genes in *Drosophila*. *Development* **125**(22): 4471-4482.

Martínez-Barberá, J.P., Toresson, H., Da Rocha, S. and Krauss, S. (1997). Cloning and expression of three members of the zebrafish Bmp family: Bmp2a, Bmp2b and Bmp4. *Gene* **198**(1-2):53-59.

Matsui,Y.,Zsebo,K.M. and Hogan, B.L. (1990). Embryonic expression of a haematopoietic growth factor encoded by the *SI* locus and the ligand for c-kit. *Nature* **347**,667-669.

McCurley,A.T. and Gallard, G.V. (2008). Characeriztion of housekeeping genes inzebrafish: male-female differences and effects of tissue type, developmental stage and chemical treatment. *BMC Molecular Biology* **9**:102.

McGinnis, W., Levine, M.S., Hafen, E., Kuroiwa, A. and Gehring, W.J. (1984). A conserved DNA sequence in homoeotic genes of the *Drosophila* Antennapedia and bithorax complexes. *Nature* **308**(5958):428-433.

McGrew, L.L., Hoppler, S. and Moon, R.T. (1997). Wnt and FGF pathways cooperatively pattern anteroposterior neural ectoderm in *Xenopus*. *Mech Dev.* **69**(1-2):105-114.

McGrew, L.L., Lai, C.J. and Moon, R.T. (1995). Specification of the anteroposterior neural axis through synergistic interaction of the Wnt signaling cascade with *noggin* and *follistatin*. *Dev Biol.* **172**(1):337-342.

Melby, A. E., Beach, C., Mullins, M. and Kimelman, D. (2000). Patterning the early zebrafish by the opposing actions of *bozozok* and *vox/vent*. *Dev.Biol.* **224**, 275-285.

Melton, D.A., Krieg, P.A., Rebagliati, M.R., Maniatis, T., Zinn, K. and Green, M.R. (1984). Efficient *in vitro* synthesis of biologically active RNA and RNA hybridization probes from plasmids containing a bacteriophage SP6 promoter. *Nucleic Acids Res* **12**(18): 7035-7056.

Mitsui, K., Tokuzawa, Y., Itoh, H., Segawa, K., Murakami, M., Takahashi, K., Maruyama, M., Maeda, M. and Yamanaka, S. (2003). The homeoprotein Nanog is required for maintenance of pluripotency in mouse epiblast and ES cells. *Cell* **113**(5):631-642.

Mullin, N.P., Yates, A., Rowe, A.J., Nijmeijer, B., Colby, D., Barlow, P.N., Walkinshaw, M.D. and Chambers, I. (2008). The pluripotency rheostat Nanog functions as a dimer. *Biochem.J.* **411**,227-231.

Narlikar, G.J., Fan, H.Y. and Kingston, R.E. (2002). Cooperation between complexes that regulate chromatin structure and transcription. *Cell* **108** (4): 475–487.

Nguyen,V.H., Schmid, B., Trout, J., Connors, S.A., Ekker, M. and Mullins, M.C. (1998). Ventral and lateral regions of the zebrafish gastrula, including the neural crest progenitors, are established by a *bmp2b/swirl* pathway of genes. *Dev Biol.* **199**(1):93-110.

Nichols, J., Zevnik, B., Anastassiadis, K., Niwa, H., Klewe-Nebenius, D., Chambers, I., Schöler, H. and Smith, A. (1998). Formation of pluripotent stem cells in the mammalian embryo depends on the POU transcription factor Oct4. *Cell* **95**(3):379-391.

Nikaido, M., Tada, M., Saji, T. and Ueno, N. (1997). Conservation of BMP signaling in zebrafish mesoderm patterning. *Mech Dev.* **61**(1-2):75-88.

Niwa, H., Miyazaki, J. and Smith, A.G. (2000). Quantitative expression of Oct-3/4 defines differentiation, dedifferentiation or self-renewal of ES cells. *Nat Genet.* **24**(4):372-376.

Nüsslein-Volhard, C. and Wieschaus, E. (1980). Mutations affecting segment number and polarity in *Drosophila*. *Nature* **287**, 795 – 801.

Nüsslein-Volhard, C., Wieschaus, E. and Kluding, H. (1984). Mutations affecting the pattern of the larval cuticle in *Drosophila melanogaster*. *Development Genes and Evolution* **193**(5): 267-282.

Postlethwait, J.H. and Schneiderman, H.A. (1969). A clonal analysis of determination in *Antennapedia* a homoeotic mutant of *Drosophila melanogaster*. *Proc Natl Acad Sci* U S A. **64**(1):176-183.

Pyati, U.J., Webb, A.E. and Kimelman, D. (2005). Transgenic zebrafish reveal stage-specific roles for Bmp signaling in ventral and posterior mesoderm development. *Development* **132**(10):2333-2343.

Ramel, M.C. and Lekven, A.C. (2004).Repression of the vertebrate organizer by Wnt8a is mediated by Vent and Vox. *Development* **131**(16): 3991-4000.

Raz, E. (2002). Primordial germ cell development in zebrafish. *Cell and Developmental Biology* **13**: 489-495.

Raz, E. (2003). Primordial germ-cell development: the zebrafish perspective. *Nat. Rev. Genet.* **4**(9):690-700.

Ryan, D.M., Matthew, B., Anthony, F., Martin, H., Martin, K., Trevor, J.P,, Helen, M., Richard, V., Steven, J.M.J. and Marco, A.M. (2008). Profiling the HeLa S3 transcriptome using randomly primed cDNA and massively parallel short-read sequencing. *BioTechniques* **45** (1): 81–94

Saffman, E.E. and Lasko, P. (1999). Germline development in vertebrates and invertebrates. *Cell Mol Life Sci.* **55**(8-9):1141-1163.

Saga, Y. (2008). Mouse germ cell development during embryogenesis. *Current Opinion in Genetics and Development* **18**(4), 337-341.

Sánchez-Sánchez, A.V., Camp, E,, Leal-Tassias, A., Atkinson, S.P., Armstrong, L., Díaz-Llopis, M. and Mullor, J.L. (2010). Nanog regulates primordial germ cell migration through Cxcr4b. *Stem Cells.* **28**(9):1457-1464.

Schier, A.F. and Talbot, W.S. (2005). Molecular genetics of axis formation in zebrafish. *Annu. Rev. Genet.* **39**:561-613.

Schmid, B., Fürthauer, M., Connors, S.A., Trout, J., Thisse, B., Thisse, C. and Mullins, M.C. (2000). Equivalent genetic roles for *bmp7/snailhouse* and *bmp2b/swirl* in dorsoventral pattern formation. *Development* 127(5):957-967.

Schulte-Merker, S, Hammerschmidt, M., Beuchle, D., Cho, K.W., De Robertis, E.M. and Nüsslein-Volhard, C. (1994). Expression of zebrafish *goosecoid* and *no tail* gene products in wild-type and mutant *no tail* embryos. *Development* **120**(4):843-852.

Schulte-Merker, S., Lee, K.J., McMahon, A.P. and Hammerschmidt, M. (1997). The zebrafish organizer requires *chordino*. *Nature* **387**, 862-863.

Scott, M.P. and Weiner, A.J. (1984). Structural relationships among genes that control development: sequence homology between the Antennapedia, Ultrabithorax, and fushi tarazu loci of *Drosophila. Proc Natl Acad Sci U S A.* **81**(13): 4115–4119.

Silva, J., Nichols, J., Theunissen, T.W., Guo, G., van Oosten, A.L., Barrandon, O., Wray, J., Yamanaka, S., Chambers, I. and Smith, A. (2009). Nanog is the gateway to the pluripotent ground state. *Cell* **138**(4):722-737.

Smith, W.C. and Harland, R.M. (1991). Injected *Xwnt-8* RNA acts early in Xenopus embryos to promote formation of a vegetal dorsalizing center. *Cell* **67**(4): 753-765.

Stachel, S.E., Grunwald, D.J. and Myers, P.Z. (1993). Lithium perturbation and *goosecoid* expression identify a dorsal specification pathway in the pregastula zebrafish.. *Development* **117**(4):1261-1274.

Stadtfeld, M. and Hochedlinger, K. (2010). Induced pluripotency: history, mechanisms, and applications. *Genes Development* **24**(20): 2239-2263.

Stickney, H.L., Imai, Y., Draper, B., Moens, C. and Talbot, W.S. (2007). Zebrafish *bmp4* functions during late gastrulation to specify ventroposterior cell fates. *Dev Biol.* **310**(1):71-84.

Sutasurya, L.A. and Nieuwkoop, P.D. (1974). The induction of the primordial germ cells in the urodeles. *Wilhelm Roux' Archiv* **175**, 199-220.

Takahashi, K., Tanabe, K., Ohnuki, M., Narita, M., Ichisaka, T., Tomoda, K. and Yamanaka, S. (2007). Induction of pluripotent stem cells from adult human fibroblasts by defined factors. *Cell* **131**(5):861-872.

Takahashi, K. and Yamanaka, S. (2006). Induction of pluripotent stem cells from mouse embryonic and adult fibroblast cultures by defined factors. *Cell* **126**, 663-676.

Tang, R., Dodd, A., Lai, D., Mcnabb, W. and Love,D.R. (2007). Validation of zebrafish *(Danio rerio)* reference genes for quantitative real-time RT-PCR normalization. **39**(5):384-390.

Thisse, C., Thisse, B., Schilling, T.F. and Postlethwait, J.H. (1993). Structure of the zebrafish *snail1* gene and its expression in wild-type, *spadetail* and *no tail* mutant embryos. *Development* **119**(4), 1203-1215.

Tissier-Seta, J.P., Mucchielli , M.L., Mark, M., Mattei, M.G., Goridis, C. and Brunet, J.F. (1995). *Barx1*, a new mouse homeodomain transcription factor expressed in cranio-facial ectomesenchyme and the stomach. *Mech Dev.* **51**(1):3-15.

Tullius, T. (1995). Homeodomains: together again for the first time. *Structure* **3**(11):1143-1145.

Vandesompele, J., De Preter, K., Pattyn, F., Poppe, B., Van Roy, N., De Paepe, A. and Speleman,F. (2002). Accurate normalization of real-time quantitative RT-PCR data by geometric averaging of multiple internal control genes. *Genome Biol* **3** (34): 1-11.

Wang, J., Levasseur, D.N. and Orkin, S.H. (2008). Requirement of Nanog dimerization for stem cell self-renewal and pluripotency. *Proc.Natl.Acad.Sci.*USA **105**, 6326-6331.

Wang, Z., Gerstein, M. and Snyder, M. (2009). RNA-Seq: a revolutionary tool for transcriptomics. *Nature Reviews Genetics* **10** (1): 57–63.

Weidinger, G., Wolke, U., Köprunner, M., Klinger, M. and Raz, E. (1999). Identification of tissues and patterning events required for distinct steps in early migration of zebrafish primordial germ cells. *Development* **126**(23):5295-5307.

Weidinger, G., Wolke, U., Köprunner, M., Thisse, C., Thisse, B. and Raz, E. (2002). Regulation of zebrafish primordial germ cell migration by attraction towards an intermediate target. *Development* **129**(1):25-36.

Wellik, D.M. (2009). *Hox* genes and vertebrate axial pattern. *Curr Top Dev Biol.* **88**:257-278.

Welstead, G.G., Brambrink, T. and Jaenisch, R.(2008) Generating iPS cells from MEFS through forced expression of Sox-2, Oct-4, c-Myc, and Klf4. *J Vis Exp* **14**, 734.

Wu,C. and Alwine, J.C. (2004). Secondary structure as a functional feature in the downstream region of mammalian polyadenylation signals. *Mol. Cell Biol.* **24** (7): 2789–2796.

Xu, L., Glass, C.K. and Rosenfeld, M.G. (1999). Coactivator and corepressor complexes in nuclear receptor function. *Curr. Opin. Genet. Dev.* **9** (2): 140–147.

Yamaguchi, S., Kurimoto, K., Yabuta, Y., Sasaki, H., Nakatsuji, N., Saitou, M. and Tada, T. (2009). Conditional knockdown of *Nanog* induces apoptotic cell death in mouse migrating primordial germ cells. *Development* **136**(23):4011-4020.

Yamaguchi, S., Kimura, H., Tada, M., Nakatsuji, N. and Tada, T. (2005). Nanog expression in mouse germ cell development. *Gene Expr. Patterns* **5**, 639–646.

Yamanaka, S. (2009). Elite and stochastic models for induced pluripotent stem cell generation. *Nature* **460**, 49-52.

Ying Y, Qi, X. and Zhao, G.Q. (2001). Induction of primordial germ cells from murine epiblasts by synergistic action of BMP4 and BMP8B signalling pathways. *Proc.Natl.Acad.Sci* U.S.A **98**(14):7858-7862.

Ying, Y., Qi, X. and Zhao, G.Q. (2002). Induction of primordial germ cells from pluripotent epiblast. *ScientificWorldJournal* **26**(2): 801-810.

Ying, Y. and Zhao, G.Q. (2001). Cooperation of endoderm-derived BMP2 and extraembryonic ectoderm-derived BMP4 in primordial germ cell generation in the mouse. *Dev Biol.* **232**(2):484-492.

Yoon, C., Kawakami, K. and Hopkins, N. (1997). Zebrafish *vasa* homologue RNA is localized to the cleavage planes of 2- and 4-cell-stage embryos and is expressed in the primordial germ cells. *Development* **124**(16): 3157-3165.

Yu, J., Hu, K., Smuga-Otto, K., Tian, S., Stewart, R., Slukvin, I. and Thomson, J. (2009). Human induced pluripotent stem cells free of vector and transgene sequences. *Science* **324**(5928): 797–801.

Yu, J., Vodyanik, M.A., Smuga-Otto, K., Antosiewicz-Bourget, J., Frane, J.L., Tian, S., Nie, J., Jonsdottir, G.A., Ruotti, V., Stewart, R., Slukvin, I.I. and Thomson, J.A. (2007). Induced pluripotent stem cell lines derived from human somatic cells. *Science* **318** (5858): 917– 1920.

Zhou, X., Sasaki, H., Lowe, L., Hogan, B.L.M. and Kuehn, M.R. (1993). *Nodal* is a novel TGF-beta-like gene expressed in the mouse node during gastrulation. *Nature* **361**: 543 – 547.

Zust, B. and Dixon, K.E. (1975). The effect of u.v. irradiation of the vegetal pole of *Xenopus laevis* eggs on the presumptive primordial germ cells. *Embryo, exp. Morph.* **34**(1): 209-220.

Materials and Methods Appendix

Construction of hsnanog-pCS2+

Polymerase Chain Reaction amplifying human *NANOG*

pEP4 E02S CK2M EN2L (5 ng/µl)	1 µl
10X Buffer for KOD Hot Start DNA Polymerase	5 µl
dNTPs (2 mM each)	5 µl
MgSO$_4$ (25 mM)	3 µl
Primer 1 (10 µM)	2 µl
Primer 2 (10 µM)	2 µl
KOD (1U/ µl)	1 µl
H$_2$O	31 µl
Total	50 µl

Typical Cycling Programme

1 = 95 °C	2	min
2 = 95 °C	20	s
3= 61 °C	10	s
4= 70 °C	15	s
5= Go to 2, 25cycles		
6= 4 °C	for ever	

Double Digestion of human *NANOG* and pCS2+ with Xho I and Xba I

	Fragment	Vector
DNA	24 µl	6.25 µl
10X NEBuffer 4	5 µl	5 µl
100X BSA	0.5 µl	0.5 µl
Xho I (20,000 U/ml)	2 µl	2 µl
Xba I (20,000 U/ml)	2 µl	2 µl
H_2O	16.5 µl	34.25 µl
Total	50 µl	50 µl

Incubate at 37 °C for 2 hours

Digestion product was purified following the QIAquick PCR Purification Protocol.

Human *NANOG* and pCS2+ ligation reaction

	Vector Only No ligase	Vector Only	Vector Insert
pCS2+Vector	6.5 µl	6.5 µl	6.5 µl
Insert	------	------	1 µl
2X Quick Ligase Buffer	10 µl	10 µl	10 µl
Quick T4 DNA Ligase	------	1 µl	1 µl
H_2O	3.5 µl	2.5 µl	1.5 µl
Total	20 ul	20 µl	20 µl

Incubate at room temperature for 5 minutes

Ligation products were used to transform competent *E coli* bacteria which were then spread on LB-agar plates containing ampicillin. Six colonies were picked from the plate spread with the ligation product of *NANOG* and pCS2+ and hsnanog-pCS2+ constructs were extracted from them. Xho I and Nco I were used to double digest the hsnanog-pCS2+ to confirm whether it was the correct construct.

Double Digestion of hsnanog-pCS2+ with Xho I and Nco I

hsnanog-pCS2+	1.5 µl
10X NEBuffer 4	2.5 µl
10X BSA	2.5 µl
Xho I	1 µl
Nco I	1 µl
H_2O	16.5 µl
Total	25 µl

Incubate at 37 °C for 2 hours

In vitro transcription of human *NANOG* mRNA

Construct hsnanog-pCS2+ was linearised by ASP718, and human *NANOG* mRNA was generated following a standard protocol of in vitro transcription.

Linearisation of hsnanog-pCS2+

hsnanog-pCS2+	12.5 µl
10XSuRE/Cut Buffer for Restriction Enzymes	5 µl
ASP718	2 µl
H_2O	30.5 µl
Total	50 µl

Incubate at 37 °C overnight

Human *NANOG* mRNA synthesis

Linearized hsnanog-pCS2+	6.1 µl
10X NEB RNA Pol Reaction Buffer	5 µl
DTT(100 mM)	5 µl
rNTPs(10mM A,C,U, 1mM G)	10 µl
Cap analogue (5mM)	5 µl
RNasin	2.5 µl
SP6 RNA polymerase	2.5 µl
H_2O	13.9 µl
Total	50 µl

Incubate at 37 °C for 30 minutes, add 2.5 µl of 5 mM GTP, incubate at 37 °C for 1 h 30 min,

add 2 µl DNase I, incubate at 37 °C for 15 min, purify RNA through SPIN column.

Construction of mnanog-pcs2+

BstX I Digestion of pMXS-Nanog

pMXS-Nanog	1 µl
10X NEBuffer 3	1 µl
10X BSA	1 µl
BstX I (10,000 U/ml)	0.4 µl
H₂O	6.6 µl
Total	10 µl

Incubate at 37 °C for 2 hours

Polymerase Chain Reaction amplifying mouse *Nanog*

pMXS-Nanog	1 µl
10X Buffer for KOD Hot Start DNA Polymerase	5 µl
dNTPs (2 mM)	5 µl
MgSO₄ (25mM)	3 µl
Primer 1 (10 µM)	2 µl
Primer 2 (10 µM)	2 µl
KOD Hot Start DNA Polymerase (1U/ µl)	1 µl
H₂O	31 µl
Total	50 µl

Typical Cycling Programme

1 = 95 °C	2 min
2 = 95 °C	20 s
3 = 61 °C	10 s
4 = 70 °C	15 s
5 = Go to 2, 25 cycles	
6 = 4 °C	For ever

Double Digestion of mouse *Nanog* and pCS2+ with BamHI and Xho I

	mNanog	pCS2+
DNA	3 µl	8 µl
10X Buffer	2.5 µl	2.5 µl
10X BSA	2.5 µl	2.5 µl
BamHI	1 µl	1 µl
Xho I	1 µl	1 µl
H$_2$O	15 µl	10 µl
Total	25 µl	25 µl

Incubate at 37 °C for 2 hours.

The digestion product was examined by gel electrophoresis, the target bands were cut out and target DNA was purified from gel slices following the QIAquick Gel Extraction Protocol.

Mouse *NANOG* and pCS2+ ligation reaction

	Vector Only	Vector Insert
pCS2+Vector	8.5 µl	8.5 µl
Insert	------	8.5 µl
10X T4 Ligase Buffer	2 µl	2 µl
T4 DNA Ligase	1 µl	1 µl
H$_2$O	8.5 µl	------
Total	20 ul	20 µl

Incubate at 16 °C overnight

Ligation products were used to transform competent *E coli* bacteria. Transformed *E.coli* bacteria were spread on LB-Agar plates containing ampicillin. Ten colonies were picked from the plate spread with the ligation product of *Nanog* and pCS2+ and mnanog-pCS2+ constructs were extracted from them. EcoR I and Xho I were used to digest the mnanog-pCS2+ to confirm whether it was the correct construct.

Double Digestion of hsnanog-pCS2+ with EcoR I and Xho I

mnanog-pCS2+	1 µl
10X NEB EcoRI Buffer	2 µl
10X BSA	2 µl
EcoR I	2 µl
Xho I	2 µl
H_2O	11 µl
Total	20 µl

Incubate at 37 °C for 2 hours

In vitro transcription of mouse *Nanog* mRNA

Construct mnanog-pCS2+ was linearised by ASP718. And mouse *Nanog* mRNA was generated following a standard protocol of in vitro transcription.

Linearisation of mnanog-pCS2+

mnanog-pCS2+	8.2 µl
10X SuRE/Cut Buffer B	5 µl
ASP718	3 µl
H_2O	33.8 µl
Total	50 µl

Incubate at 37 °C overnight

Mouse *Nanog* mRNA synthesis

Linearised mnanog-pCS2+	8 µl
10X RNA Pol Reaction Buffer	5 µl
DTT (100 mM)	5 µl
rNTPs (10mM A,C,U, 1Mm G)	10 µl
Cap analogue (5mM)	5 µl
RNasin	2.5 µl
RNA polymerase	2.5 µl
H_2O	12 µl
Total	50 µl

Incubate at 37 °C for 30 minutes, add 2.5 µl of 5 mM GTP, incubate at 37 °C for 1 h 30 min,

add 2 µl DNase I, incubate at 37 °C for 15 min, purify RNA through SPIN column.

Total RNA extraction and reverse transcription

Total RNA extraction from embryos

Collect embryos in eppendorfs, remove as much liquid as possible and freeze on dry ice. Store at -80 °C. Add 500 µl TRIZOL and homogenise embryos (using eppendorf pestle). Incubate at 65 °C for 10 minutes.

Spin phase lock tubes at 13 krpm for 1 min. transfer homogenate to Phase-lock tubes. Add 100 µl chloroform, shake (do not vortex), and spin at 12 krpm for 10 min.

Transfer upper aqueous phase to new tube. Add 300 µl isopropanol and mix by inversion. Incubate at room temperature for 10 min. Spin at 13 krpm for 10 min at 4 °C. Discard supernatant, add 70% ethanol, and vortex briefly. Spin at 13 krpm for 5 min for 4 °C. Discard supernatant, air dry for 5 min, resuspend in 88 µl ddH$_2$O.

Add 10 µl DNase Buffer 10X and 2 µl DNase I (RNase-free). Incubate at 37 °C for 1 hour. Take 2 µl and run on 1% gel to check quality of RNA.

Add 102 µl ddH$_2$O. Add 200 µl Phenol:Chloroform:isoamyl alcohol, vortex and spin at 13 krpm for 5 min. Transfer aqueous phase to new tube, add 200 µl isopropanol and mix by inversion. Spin at 13 krpm for 10 min at 4 °C. Discard supernatant, add 200 µl 70% ethanol and spin at 13 krpm for 5 min. Discard supernatant, air dry for 5 min, and resuspend in 20 µl ddH$_2$O. Determine yield by spectrophotometer.

Reverse transcription

Mix together the following:

RNA (1 µg)

Random primer (250 ng)

H_2O

	_____
Total	12 µl

Incubate at 65 °C for 10 min. Transfer tube straight onto ice and leave for 2 min.

Add   5X First strand buffer   4 µl

     DTT (100 mM)   2 µl

     dNTPs (10 mM)   1 µl

Incubate at 25 °C for 2 min. Add 1 µl SuperScriptII Reverse Transcriptase and mix. Incubate at 25 °C for 10 min. Incubate at 42 °C for 50 min. Incubate at 70 °C for 10 min. Make up to 100 µl with H_2O and use 1 µl for PCRs.

PCR reaction to amplify *beta-actin* from cDNA

cDNA	1 μl
10X Buffer for Hot Start Polymerase	1 μl
dNTPs (2 mM)	0.2 μl
$MgSO_4$ (25 mM)	0.2 μl
Primers (10 μM)	0.4 μl
KOD Hot Start Polymerase(1U/ μl)	1 μl
H_2O	5.4 μl
Total	10 μl

Thermal Cycling Program

1 = 94 °C	120 s
2 = 94 °C	20 s
3= 60 °C	20 s
4= 72 °C	30 s
5= Go to 2, 35cycles	
6= 4°C	for ever

Results Appendix

Construction of hsnanog-pCS2+
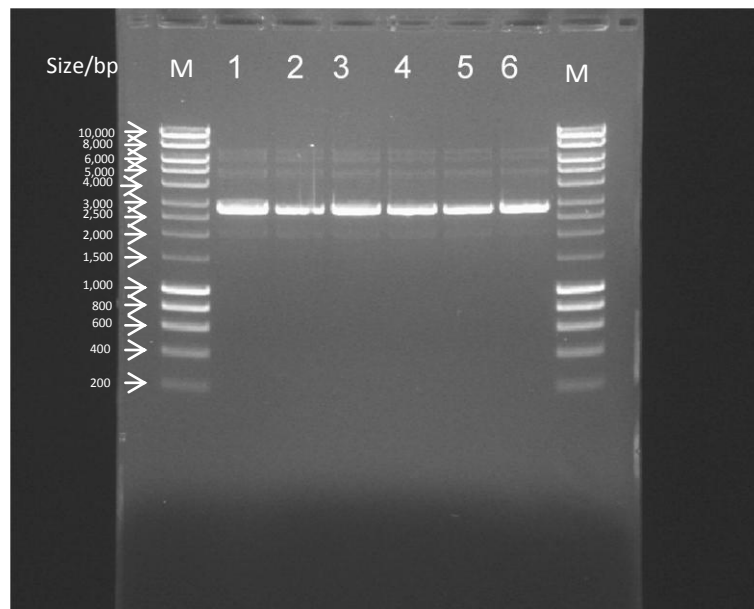
Figure S1.hsnanog- pCS2+

1-6, Uncut hsnanog-pCS2+ constructs 1-6. M, Marker Hyperladder I. In lanes 1-6 are bands of uncut hsnanog-pCS2+ plasmids.   The pattern of bands in each lane is the same. There are four bands in each lane, representing distribution of plasmid conformations. The brightest band representing supercoiled plasmid is near where 3 kb marker DNA is. Nicked and linear plasmids run slower than supercoiled, located near 5 kb and 7 kb marker DNA, respectively. Denatured supercoiled plasmid runs faster than supercoiled, almost as fast as 2 kb marker DNA.

Construction of mnanog-pcs2+
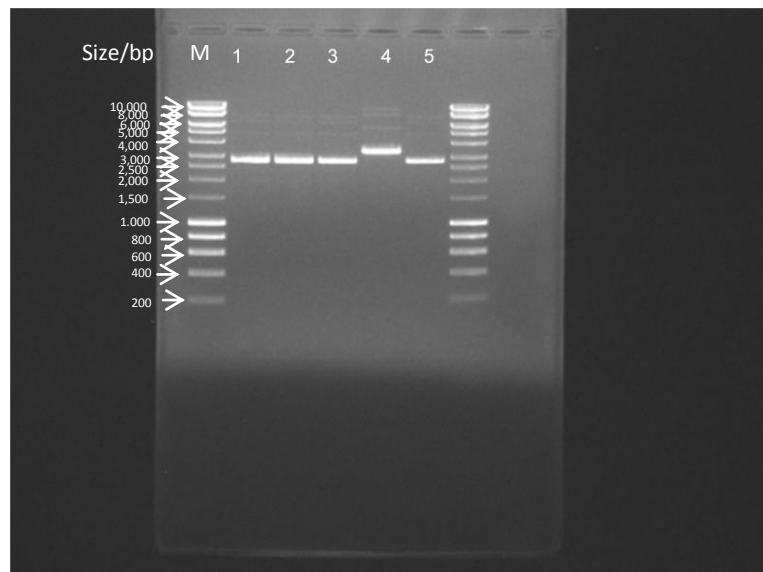
Figure S2. mnanog-pCS2+ 1-5

M, Hyperladder I. 1-5, mnanog-pCS2+ 1-5. In lanes 1-5 are bands of mnanog-pCS2+ plasmids. There are about four bands in each lane. The pattern of the bands in all these lanes is the same except that of the lane 4, which run slower. In lanes 1-3 and 5, the brightest band representing supercoiled plasmid is near 3 kb marker DNA. Nicked and linear plasmid runs almost as fast as 5 kb and 7 kb marker respectively. The slowest band near 8 kb marker DNA may represent dimers and multimers of plasmid. In lane 4, the supercoiled plasmid is near 4 kb marker DNA.   The other three slower bands are near 6 kb, 8 kb and 9 kb marker DNA respectively.
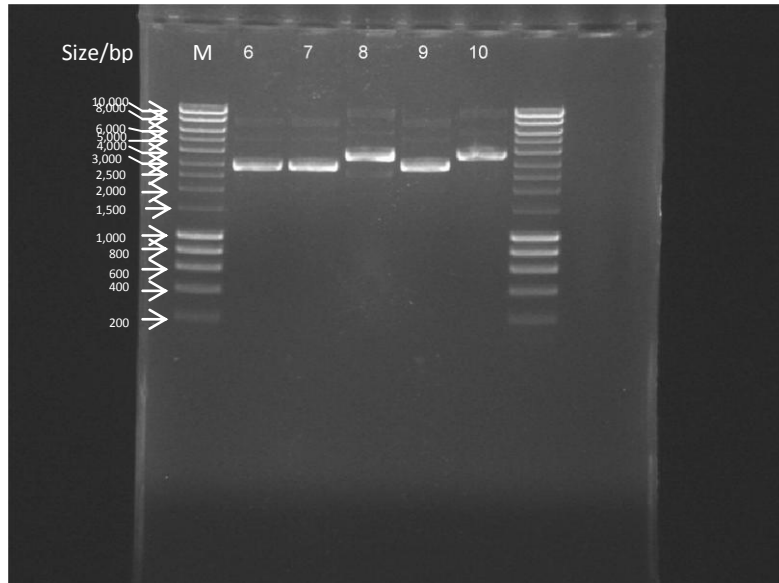
Figure S3. mnanog-pCS2+ 6-10

M, Marker Hyperladder I. 6-10, mnanog-pCS2+ 6-10. In lanes 6-10 are bands of mnanog-pCS2+ plasmids. Lanes 6, 7 and 9 have the same band pattern while the other two lanes 8 and 10 share another type of bands which run slower. In lanes 6, 7 and 10, the brightest band representing supercoiled plasmid is near 3 kb marker DNA. Nicked and linear plasmids run slower and are near 5 kb and 8 kb marker DNA. In lanes 8 and 10, the brightest supercoiled band runs almost as fast as 4 kb marker DNA does. The other two bands, representing nicked and linear plasmid, are near 6 kb and 10 kb marker DNA.

Quantitative RT-PCR

Standard curves

Standard curves yielded by a plot of log 10 of quantities of *chordin*, *squint*, *goosecoid* ,*wnt8a*, *bmp2b* and *bactin* against Ct in a series of diluted cDNA mix (undiluted, 1 in4, 1 in 16, 1 in 64, 1in 256, and 1 in 1024) of three replicates of uninjected control embryos
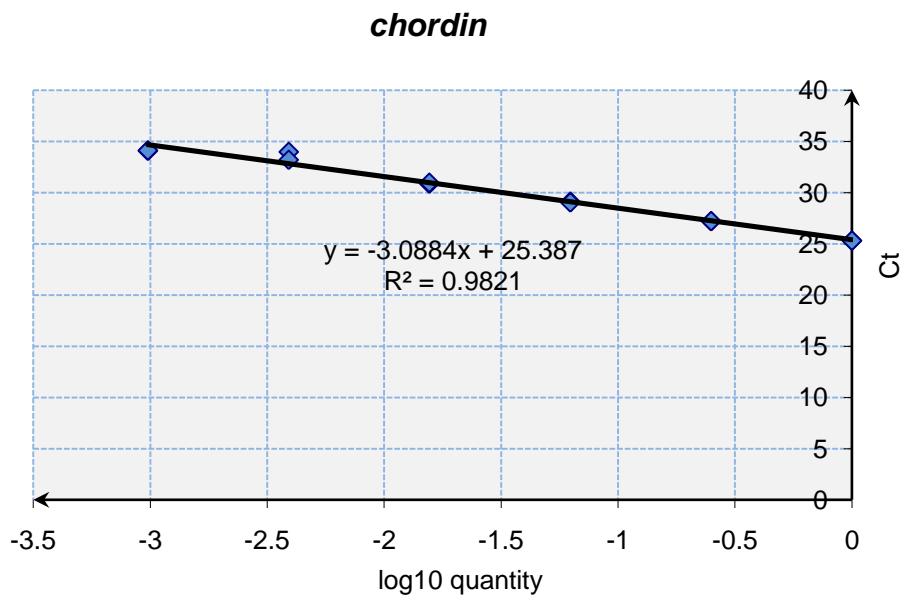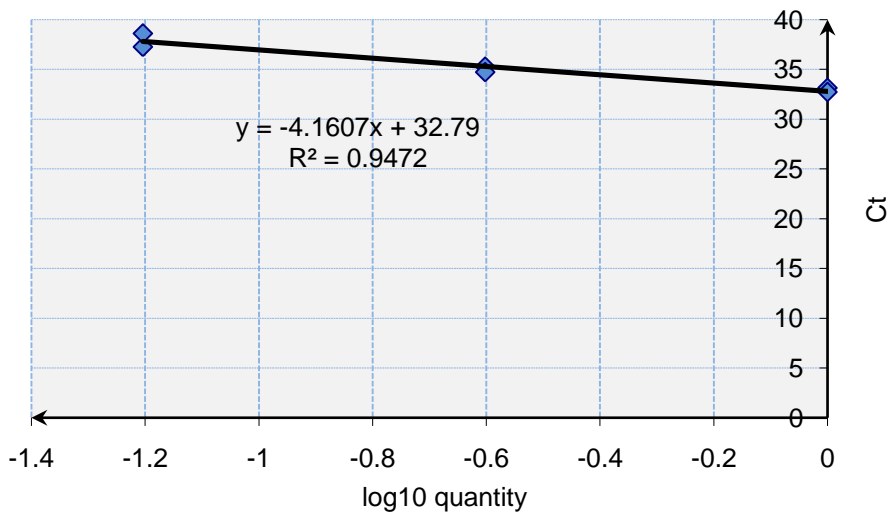
chordin

$$y = -3.0884x + 25.387$$
$$R^2 = 0.9821$$

squint

$y = -4.1607x + 32.79$
$R^2 = 0.9472$

log10 quantity

goosecoid

$y = -3.0827x + 27.324$
$R^2 = 0.985$

log 10 Quantity

92

wnt8a

$$y = -3.1813x + 29.332$$
$$R^2 = 0.9794$$

log10 quantity

Ct

bmp2b

$$y = -3.5352x + 24.367$$
$$R^2 = 0.9658$$

log 10 Quantity

Ct

bactin

$$y = -3.6745x + 21.18$$
$$R^2 = 0.9892$$
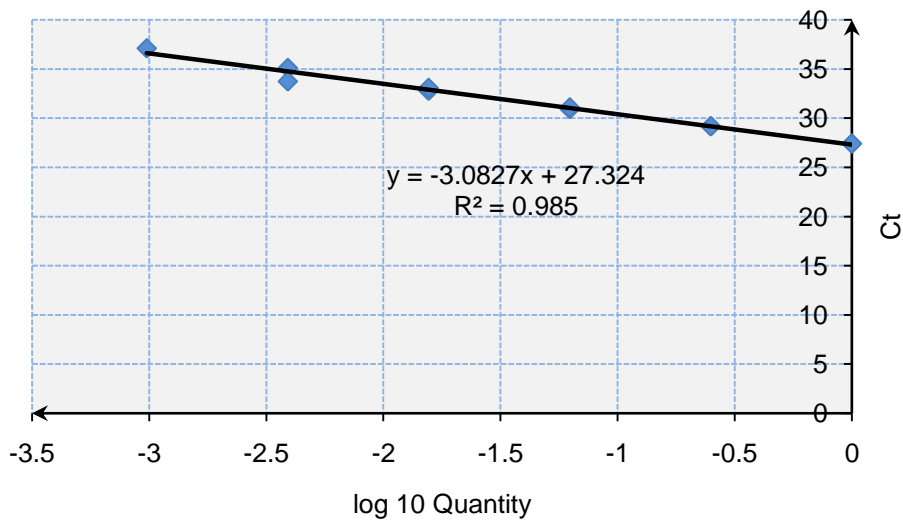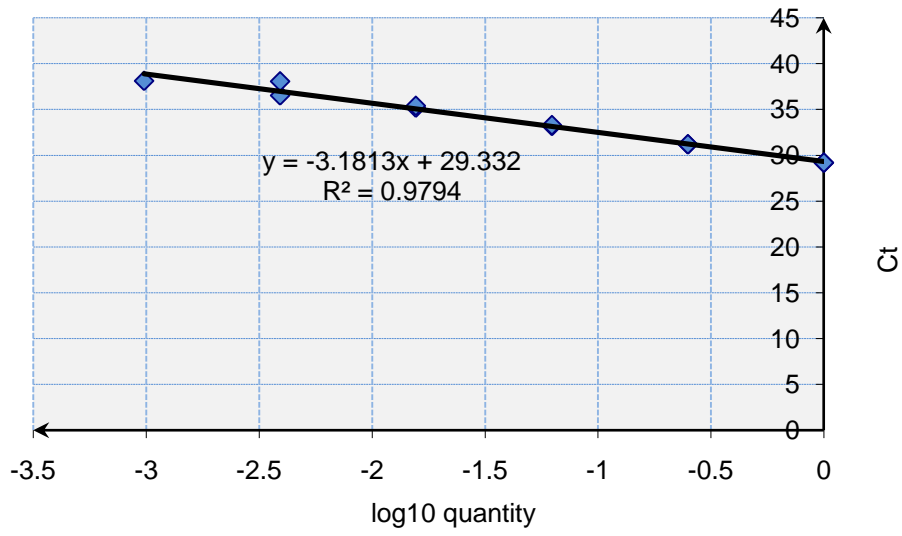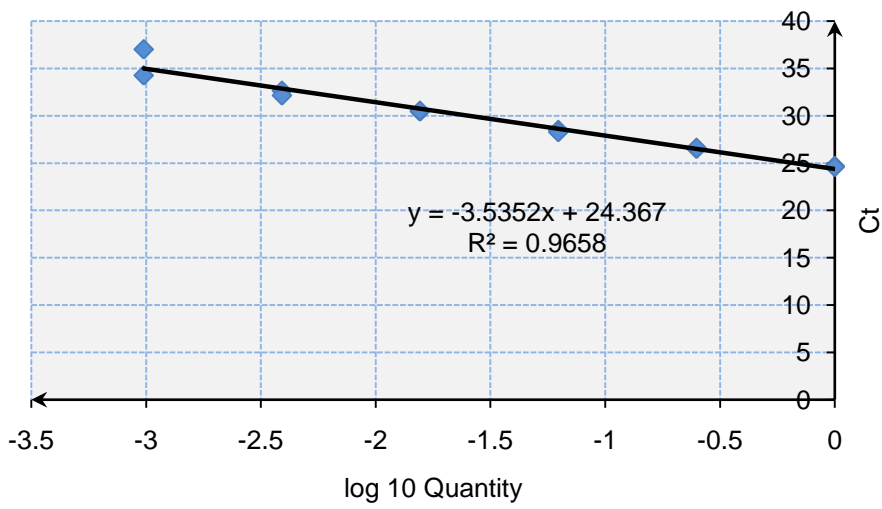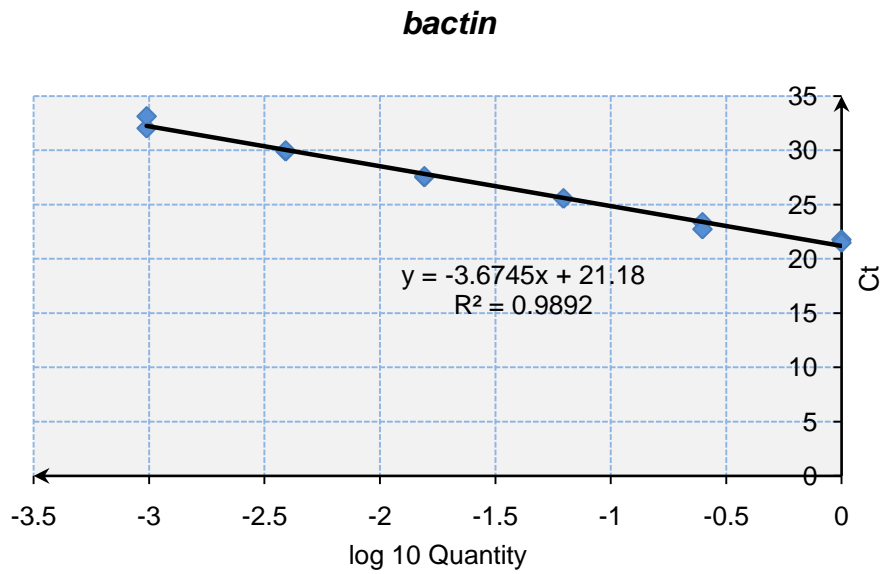
Ct and Quantities of *chordin, squint, goosecoid, wnt8a, bmp2b* and *beta-actin*

Ct and Quantities of *chordin,squint, goosecoid ,wnt8a, bmp2b* and *beta-actin* in *NANOG/Nanog-*injected embryos and uninjected control embryos. un1, un2 and un3 represent three replicates of uninjected control embryos. inj1, inj2 and inj3 are replicates of embryos injected with human *NANOG*, while inj4, inj5 and inj6 are replicates injected with mouse *Nanog*.

chordin

		Ct	Quantity
un1	zf chd	24.88	1.46
un1	zf chd	24.71	1.66
un2	zf chd	25.09	1.25
un2	zf chd	25.14	1.21
un3	zf chd	25.38	1.01
un3	zf chd	25.33	1.04
inj1	zf chd	24.27	2.31
inj1	zf chd	24.23	2.38
inj2	zf chd	24.81	1.54
inj2	zf chd	24.84	1.5
inj3	zf chd	25.13	1.21
inj3	zf chd	25.05	1.28
inj4	zf chd	26.21	5.43E-01
inj4	zf chd	26.2	5.45E-01
inj5	zf chd	26.43	4.59E-01
inj5	zf chd	26.43	4.61E-01
inj6	zf chd	25.82	7.26E-01
inj6	zf chd	25.83	7.21E-01

squint

		Ct	Quantity
un1	sf sqtutr	31.94	1.6
un1	sf sqtutr	31.8	1.73
un2	sf sqtutr	32.72	1.04
un2	sf sqtutr	32.37	1.26
un3	sf sqtutr	32.85	9.63E-01
un3	sf sqtutr	33.44	6.96E-01
inj1	sf sqtutr	32.28	1.33
inj1	sf sqtutr	32.53	1.15
inj2	sf sqtutr	32.25	1.35
inj2	sf sqtutr	33.01	8.84E-01
inj3	sf sqtutr	32.22	1.37
inj3	sf sqtutr	32.16	1.41
inj4	sf sqtutr	32.76	1.01
inj4	sf sqtutr	33.22	7.85E-01
inj5	sf sqtutr	33.99	5.15E-01
inj5	sf sqtutr	33.48	6.82E-01
inj6	sf sqtutr	32.85	9.65E-01
inj6	sf sqtutr	33.16	8.15E-01

goosecoid

			Ct	Quantity
un1	Zf gsc		27.03	1.25
un1	Zf gsc		27.16	1.13
un2	Zf gsc		27.42	0.933
un2	Zf gsc		27.43	0.926
un3	Zf gsc		27.53	0.857
un3	Zf gsc		27.59	0.819
inj1	Zf gsc		25.57	3.72
inj1	Zf gsc		26.07	2.56
inj2	Zf gsc		26.15	2.41
inj2	Zf gsc		26.23	2.26
inj3	Zf gsc		26.33	2.1
inj3	Zf gsc		27.61	0.806
inj4	Zf gsc		28.61	0.383
inj4	Zf gsc		28.14	0.546
inj5	Zf gsc		27.99	0.607
inj5	Zf gsc		28.66	0.369
inj6	Zf gsc		26.99	1.29
inj6	Zf gsc		26.65	1.65

wnt8a

		Ct	Quantity
un1	Zfwnt8a	28.57	1.74
un1	Zfwnt8a	28.6	1.69
un2	Zfwnt8a	29.38	9.68E-01
un2	Zfwnt8a	29.42	9.41E-01
un3	Zfwnt8a	29.82	7.02E-01
un3	Zfwnt8a	29.89	6.69E-01
inj1	Zfwnt8a	29.92	6.55E-01
inj1	Zfwnt8a	29.96	6.37E-01
inj2	Zfwnt8a	31.03	2.94E-01
inj2	Zfwnt8a	30.87	3.29E-01
inj3	Zfwnt8a	30.89	3.23E-01
inj3	Zfwnt8a	31.15	2.68E-01
inj4	Zfwnt8a	31.29	2.43E-01
inj4	Zfwnt8a	31.19	2.60E-01
inj5	Zfwnt8a	32.55	9.73E-02
inj5	Zfwnt8a	32.77	8.29E-02
inj6	Zfwnt8a	32.16	1.29E-01
inj6	Zfwnt8a	32.13	1.32E-01

bmp2b

		Ct	Quantity
un1	Zfbmp2	23.96	1.3
un1	Zfbmp2	24.01	1.26
un2	Zfbmp2	24.22	1.1
un2	Zfbmp2	24.34	1.02
un3	Zfbmp2	24.66	0.824
un3	Zfbmp2	24.51	0.913
inj1	Zfbmp2	24.29	1.05
inj1	Zfbmp2	24.12	1.18
inj2	Zfbmp2	24.64	0.838
inj2	Zfbmp2	24.46	0.944
inj3	Zfbmp2	24.26	1.07
inj3	Zfbmp2	25	0.663
inj4	Zfbmp2	25.35	0.528
inj4	Zfbmp2	25.43	0.501
inj5	Zfbmp2	25.37	0.519
inj5	Zfbmp2	25.52	0.473
inj6	Zfbmp2	24.95	0.684

bactin

un1	zfbact	20.9	1.19
un1	zfbact	20.86	1.22
un2	zfbact	21.35	0.901
un2	zfbact	21.33	0.913
un3	zfbact	21.4	0.874
un3	zfbact	21.38	0.882
inj1	zfbact	20.59	1.45
inj1	zfbact	20.74	1.32
inj2	zfbact	21.32	0.915
inj2	zfbact	21.41	0.867
inj3	zfbact	21.71	0.72
inj3	zfbact	21.63	0.756
inj4	zfbact	22.65	0.398
inj4	zfbact	22.68	0.39
inj5	zfbact	22.8	0.363
inj5	zfbact	22.69	0.389
inj6	zfbact	21.92	0.631
inj6	zfbact	21.94	0.62

T-tests

T-tests with two samples assuming unequal variances were performed to compare *chordin*, *squint*, *goosecoid, wnt8a* and *bmp2b* expression in *NANOG*/*Nanog*-injected embryos with that in uninjected control embryos.   UNINJ: uninjected control embryos; INJ: *NANOG*/*Nanog*-injected embryos

chordin

	UNINJ	INJ
Mean	1.272717	1.474478
Variance	0.009261	0.063877
Observations	3	6
Hypothesized Mean Difference	0	
df	7	
t Stat	-1.72169	
P(T<=t) one-tail	0.064399	
t Critical one-tail	1.894579	
P(T<=t) two-tail	0.128799	
t Critical two-tail	2.364624	

squint

	UNINJ	INJ
Mean	1.19814	1.55416
Variance	0.05139	0.235064
Observations	3	6
Hypothesized Mean Difference	0	
df	7	
t Stat	-1.50035	
P(T<=t) one-tail	0.088605	
t Critical one-tail	1.894579	
P(T<=t) two-tail	0.17721	
t Critical two-tail	2.364624	

goosecoid

	UNINJ	INJ
Mean	1	2.050471
Variance	0.001818	0.383778
Observations	3	6
Hypothesized Mean Difference	0	
df	5	
t Stat	-4.13402	
P(T<=t) one-tail	0.004525	
t Critical one-tail	2.015048	
P(T<=t) two-tail	0.009049	
t Critical two-tail	2.570582	

wnt8a

	UNINJ	INJ
Mean	1.085453	0.383838
Variance	0.104018	0.024905
Observations	3	6
Hypothesized Mean Difference	0	
df	2	
t Stat	3.560843	
P(T<=t) one-tail	0.035307	
t Critical one-tail	2.919986	
P(T<=t) two-tail	0.070615	
t Critical two-tail	4.302653	

bmp2b

	UNINJ	INJ
Mean	1	1.039978
Variance	0.007073	0.033214
Observations	3	6
Hypothesized Mean Difference	0	
df	7	
t Stat	-0.44998	
P(T<=t) one-tail	0.333164	
t Critical one-tail	1.894579	
P(T<=t) two-tail	0.666329	
t Critical two-tail	2.364624	